Flow condensation heat transfer performance of natural and emerging synthetic refrigerants

Jordan A. Morrow[#,1], Ryan A. Huber[#,1], Kashif Nawaz[2,*], Melanie M. Derby[1]

[1]Kansas State University, 3002 Rathbone Hall, 1701B Platt St., Manhattan, KS 66506, USA

[2]Oak Ridge National Laboratory, Building 3147, One Bethell Valley Rd., Oak Ridge, TN 37931, USA

[#]co-first authors

[*]corresponding author nawazk@ornl.gov, tel. +1 865-241-0972, fax +1 865-574-9338

Abstract

There is great interest in predicting flow condensation heat transfer for lower global warming potential (GWP) fluids. This paper analyzes the efficacy of common flow condensation correlations developed for particular fluids in order to identify their suitability to predict heat transfer performance of low GWP fluids. Condensation heat transfer data were extracted from the literature, including 19 papers and 1,473 data points for natural refrigerants [i.e., ammonia (R717), CO_2 (R744), propane (R290), isobutane (R600a)] and 35 papers and 5,030 data points for synthetic refrigerants [i.e., R12, R1234yf, R1234ze(E), R1234ze(Z), R22, R32, R41, R123, R125, R134a, R142b, R152a, R161, R404A, R410A, R448A, R449A, R450A, R452B, R454C, R455A, R513A] encompassing tube diameters of 0.1–11.5 mm, mass fluxes of 55–1200 kg/m^{2}s, and saturation temperatures of -25ºC–65ºC. Correlations analyzed included Akers et al. (1959), Cavallini et al. (2006, 2011), Kim and Mudawar (2013), Macdonald and Garimella (2016), Shah (1979, 2009, 2013, 2016) and Traviss et al. (1973) for smooth tubes and Chamra et al. (2005) and Kedzierski and Goncalves (1999) for enhanced tubes. Since most studies did not report wall temperature, correlations which relied on wall temperature directly or indirectly were excluded from the analysis. For synthetic refrigerants, mean average error (MAE) ranged from 6%–257%, and Cavallini et al. (2011) and Kim and Mudawar (2013) were the best predictors for emerging

synthetic refrigerants. The Kim and Mudawar (2013) correlation was found to best predict the heat transfer performance for propane and R600a data, but most correlations did not accurately predict ammonia and CO_2 flow condensation.

Keywords: refrigerants, condensation, low global warming potential, low GWP, correlation, minichannels

Nomenclature

Symbol	Name	Units
A	Coefficient	-
B	Coefficient	-
c_p	Specific heat	J $kg^{-1}K^{-1}$
D	Diameter or hydraulic diameter	m
e	Microfin height	m
E	Entrainment ratio	-
f	Friction factor	-
Fr	Froude number	-
g	Gravitational acceleration	m s^{-2}
G	Mass flux, mass flow rate divided by area	kg $m^{-2}s^{-1}$
Ga	Galileo number	-
h	Heat transfer coefficient	W $m^{-2}K^{-1}$
j	Superficial velocity	m s^{-1}
k	Fluid thermal conductivity	W $m^{-1}K^{-1}$
MAE	Mean average error	%
Nu	Nusselt number	-
p	Pressure	Pa
Pr	Prandtl number	-
Re	Reynolds number	-
Rx	Microfin empirically fitted relative roughnees	-
Su	Suratman number	-
Sv	Nondimensional specific volume	-
T	Temperature	^oC or K
u	Velocity	m s^{-1}
u^*	Friction velocity	-
We^*	Modified Weber number	-
x	Quality	-
X	Lockhart Martinelli parameter	-
y	Length scale perpendicular to channel wall	m
Z	Shah's correlation parameter	-
β	Microfin apex angle	^{o}
δ	Liquid film thickness	m or -

ε	Void fraction	-
θ	Stratification angle	Rad
κ	Heat transfer enhancement factor	-
μ	viscosity	Pa s
ξ	Liquid fraction in upper film	-
ρ	Liquid density	kg m^{-3}
σ	Surface tension	N m^{-1}
τ	Shear stress	Pa
Subscripts		
c	Critical	
E	Entrainment	
ff	Falling film	
i	Interfacial	
ls	Assuming liquid phase flowing alone	
l	Liquid	
lf	Liquid film	
lo	Liquid only, assumes all mass flowing as a liquid	
r	Reduced pressure (i.e., p/p_c)	
sat	Saturation temperature	
tt	Turbulent liquid, turbulent vapor	
ulf	Upper liquid film	
v	Vapor	
vo	Vapor only, assumes all mass flowing as a vapor	
w	Wall	
Superscripts		
+	Nondimensional turbulent parameter	

2. Introduction

The selection of refrigerants for specific engineering applications depends on the required engineering constraints (e.g., operating temperatures and pressures, capacity, latent heat of vaporization) and evolving environmental regulations. The Montreal Protocol, a multi-national treaty signed in 1987, was designed to eliminate the usage of fluids with unacceptable ozone depletion potential (ODP) such as chlorofluorocarbons (CFCs), prompting the phase out of common conventional refrigerants (e.g., R-11, R-12, R-22, R-123, etc.) [1]. Developing countries with "controlled substances in Annex A is less than 0.3 kilograms per capita" were bound by

Article 5 of the agreement, which described a slower phaseout timeline [1]. The Montreal Protocol successfully phased out 99% of ODP substances [1].

Amendments to the Montreal Protocol were signed in Kigali, Rwanda in 2016 with the goal of reducing 80% of hydrofluorocarbons (HFCs) to prevent up to 0.4°C of global warming. These reductions are expected to proceed according to three different timelines, starting in 2019 for non-Article 5 countries and 2024 and 2028 for two groups of Article 5 countries [1-3]. In conjunction with the Paris Climate Agreement's efforts to limit global warming to 1.5 ^{o}C [3], the second round of refrigerant phaseouts affects commonly-used HFC refrigerants (e.g., R134a, R404A, R410A, etc.). New technology development is essential to meeting the Kigali Amendments phase-out plan in a cost-effective manner, including increasing energy efficiency of systems with zero ODP and lower global warming potential (GWP) alternative refrigerants [4]. Europe's F-gas regulations limit automotive refrigeration to fluids with GWP less than 150, thereby favoring natural refrigerants which often have lower GWPs [5]. Table 1 presents a summary of several refrigerants and their attributes which have been considered for typical HVAC&R applications.

Table 1 Characteristics and environmental impact of different refrigerants

Refrigerant group	Refrigerant example	ODP	GWP_{100}	Atmospheric lifetime (years)	Flammability
CFCs	R11, R12, R115	0.6–1	4,750–14,400	45–1,700	Nonflammable
HCFCs	R22, R141b, R124	0.02–0.11	400–1,800	1–20	Nonflammable
HFCs	R407C, R32, R134a	0	140–11,700	1–300	Nonflammable or mildly flammable
HFOs	R1234yf, R1234ze, R1234yz	0	0–12	-	Mildly flammable
Natural refrigerants	CO_2/R744, Ammonia/R717, HC (Propane/R290, R600, R600a)	0	0	Few days	HCs: Highly flammable R717: Flammable R744: Nonflammable

Refrigerants such as hydrocarbons, ammonia and CO_2 have emerged as potential replacements for refrigerants with higher GWP. While they have been used for many years in certain applications, all three alternatives have major technical and safety demerits for which they cannot have widespread implementation without appropriate safety measures. For example, ammonia is toxic and mildly flammable and has been classified as B2L [5, 6]. Similarly, hydrocarbons have flammability concerns and the deployment rate is slow due to safety regulations. CO_2 is unique in its operating conditions and has shown great performance for low temperature heat pump applications but the operating pressure for trans-critical CO_2 requires a mechanically strong infrastructure to withstand mechanical stresses [7]. Regardless of these disadvantages, all three refrigerants have been extensively deployed in commercial and industrial refrigeration. Propane and CO_2 based heat pumps are commercially available. An alternative solution has been provided by synthetic refrigerants including hydroflouroolefins (HFOs) and their blends, offering a middle option when having to balance between GWP and flammability.

Several existing studies have shown that these working fluids are suitable replacement to existing refrigerants with higher GWP and often do not require substantial modification to the baseline system. Refrigerants (e.g., R1234yf, R1234ze(E), R32, R452B, etc.) have been classified as A2L due to their mild flammability and despite this have extensive interest for residential air conditioning and heat pump applications [8, 9]. The cost of these refrigerants is noticeably higher compared to the conventional fluids (i.e., up to 10 times greater). Both safety and cost concerns have established the need to better understand the heat transfer process for refrigerants in tubes and microchannels to decrease the amount of working fluid in the system. Due to their recent emergence, the thermal-hydraulic behavior of these working fluids is not well understood. To

mitigate these issues, an effort has been made on deploying heat exchangers (condensers and evaporators) which can result in reduced refrigerant charge. Two obvious options in this regard are round tube heat exchangers deploying smaller diameter tubes (5 mm or smaller) and micro-channel heat exchangers.

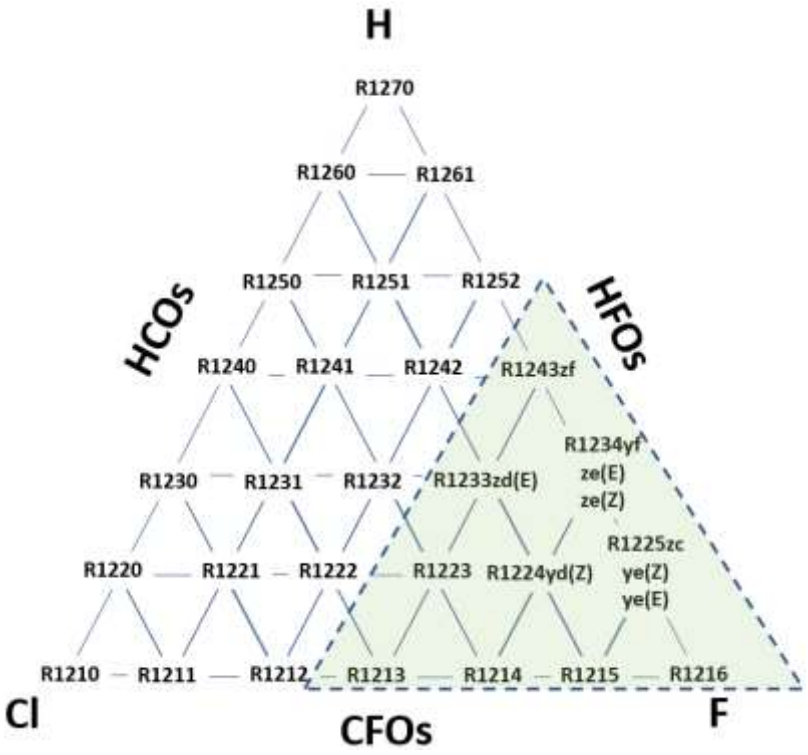

Figure 1 Emerging refrigerants- Working fluids in green triangle have been considered for various applications

Heat exchangers are critical components of the typical HVAC&R systems since they account for more than 50% of the energy required to provide the heating or cooling performance [10]. Condensers account for at least 40% of the refrigerant in the system (there are exceptions for variable flow rate (VRF) systems) and has been extensively studied [8, 9]. For example, in a typical heat pump water heater, almost 60% of the refrigerant resides in a wrapped condenser. Due to the impact on performance and charge requirement, it is important to analyze the flow behavior in the condenser channels. Commercial equipment manufacturers have been relying on existing

performance correlations for in-tube flow condensation to develop the model for the performance of the condenser which eventually establishes the performance for the overall system. As such, an accurate assessment of the heat transfer behavior is mandatory. While the existing correlations for in-tube condensation have been developed over the years, most of these correlations represent individual efforts which are often focused on selective refrigerants, specific tube designs, and flow conditions. The error associated with such correlations is also relatively large due to the very nature of two-phase flow and associated uncertainties in experimental measurements. This scenario has caused challenges for practicing engineers and researchers who must become familiar with all background information to know if a particular performance correlation can be used effectively. The current study is focused on providing a resolution to this continued challenge. A comprehensive review of the existing low GWP and natural refrigerant literature has been presented and the representative data has been acquired for various studies. Most data collection ended June 2020. Then the extensive data set has been used to make a comparison of various performance correlations and discrepancies have been identified.

The research objectives of this paper are to: 1) identify studies which present experimental data for in-tube condensation, 2) compare heat transfer coefficients, and 3) assess correlations for use with natural and synthetic low GWP refrigerants.

3. Literature review focusing on in-tube flow condensation with refrigerants

3.1 Synthetic refrigerants

Table 2 summarizes the experimental data on low GWP, synthetic refrigerants found in the literature, including correlations used to predict experimental data in the original papers. Some refrigerants have heat transfer coefficient data covering a wide range of diameters, mass fluxes, temperatures, and qualities, while others have limited range of parameters. Low GWP synthetic

alternative refrigerants can be placed in one of three categories—HFOs [e.g., R1234yf, R1234ze(E)], low GWP HFCs (e.g., R152a, R161), and HFC/HFO mixtures (e.g., R452B, R513A). Each of these categories has their own inherent demerits in terms of environmental impacts and safety concerns. The two most common HFOs, R1234yf and R1234ze(E), have a considerable amount of data available in literature (e.g., 452 data points from 9 papers and 919 data points from 16 papers, respectively). R1234yf focused studies include range of data with diameters varying from 0.71 to 8 mm, mass fluxes ranging from 100–1,200 kg $m^{-2}s^{-1}$ with an average of 471 kg $m^{-2}s^{-1}$, and temperatures ranging from 15°C–60°C with an average of 36.4°C [11-19]. R1234ze(E) focused studies have data with diameters ranging from 0.85–6.1 mm, mass fluxes ranging from 55–1,000 kg $m^{-2}s^{-1}$ with an average of 329 kg $m^{-2}s^{-1}$, and temperatures ranging from 29°C–65°C with an average of 39°C [13, 14, 18, 20-31]. Limited experimental data is available for remaining HFOs except for R1234ze(Z), which is another isomer of R1234ze [32]. R1234ze(Z) data are limited to microfin tubes (e.g., 41 data points from 1 paper) and has one tube diameter, i.e., 5.35 mm, mass fluxes ranging between 150 and 400 kg $m^{-2}s^{-1}$ with an average of 284 kg $m^{-2}s^{-1}$, and temperatures ranging from 37°C to 65°C with an average of 63.4°C [31]. Rignetti et al. [32] conducted a critical review on boiling and condensing for HFOs [33]. For condensation, the review compared predictive models; only a couple of which are studied in this paper [34, 35] and some used wall temperature [36-41].

Some low GWP HFCs (i.e., R32 and R152a) have a large amount of data (1,122 data points from 22 papers and 312 data points from 5 papers, respectively) since they were also considered during the phase out of CFCs and HCFCs. The R32 data covers a range of diameters (i.e., 0.85–11.5 mm), and the R152a data covers a similar diameter range (i.e., 0.952–9.64 mm). R32 data covers mass fluxes between 55–1,200 kg $m^{-2}s^{-1}$ with an average of 309 kg $m^{-2}s^{-1}$ and temperatures

between 30°C–50°C with an average of 39.2°C [11, 13, 16, 20-25, 27-30, 42-49]. R152a data covers mass fluxes between 75–800 kg $m^{-2}s^{-1}$ with an average of 328 kg $m^{-2}s^{-1}$ and temperatures between 30–50°C with an average of 38°C [14, 28, 44, 47, 50]. Other low GWP HFCs such as R161 and R41 have limited data both in quantity and range—45 data points from 1 paper and 38 data points from 1 paper, respectively. The R161 data covers a mass flux range of 200–400 kg $m^{-2}s^{-1}$ with an average of 267 kg $m^{-2}s^{-1}$ and a temperature range of 35°C–45°C with an average of 36.7°C [24]. The R41 data covers a mass flux range of 200–400 kg $m^{-2}s^{-1}$ with an average of 279 kg $m^{-2}s^{-1}$ and a temperature range of 35–40°C with an average of 35.7°C [24].

HFC/HFO refrigerants have emerged as an alternative to high GWP HFC refrigerants that could help with the transition as a step toward low GWP refrigerants or as a permanent alternative in some cases. Either way, many of these mixtures exist now, though they are not represented with heat transfer coefficient data. Many of these alternatives were studied in drop-in replacement studies, but they are significantly lacking in condensation heat transfer coefficient data. While it is important to know how these new refrigerants perform in systems, fundamental condensation heat transfer coefficient data are important for heat exchanger design and simulations. Only a handful of HFC/HFO refrigerants have heat transfer coefficient data and only a few studies on each of the refrigerants that have been tested. R447A data was tested in 1 paper (54 data points) in one diameter (0.86 mm). R447A data have mass fluxes ranging between 100–300 kg $m^{-2}s^{-1}$ with an average of 200 kg $m^{-2}s^{-1}$ and temperatures between 35–45°C with an average of 40°C [22]. The R447A data were not used in the correlation analysis due to lack of proper property tables. R448A and R449A were tested in 1 paper (15 data points and 14 data points, respectively). They were tested in a mass flux range of 100–400 kg $m^{-2}s^{-1}$, one temperature (i.e., 45°C), and one diameter (i.e., 5.6 mm). R450A has only been tested in one diameter, i.e., 4.7 mm, by one paper (106 data

points). R450A data have mass fluxes ranging between 100–550 kg $m^{-2}s^{-1}$ with an average of 369 kg $m^{-2}s^{-1}$, and temperatures between 45°C–55°C with an average of 49.6°C [51]. R452B (100 data points) was studied by one research group in two different diameters (i.e., 0.96 mm and 8 mm). R452B data have mass fluxes ranging between 100–800 kg $m^{-2}s^{-1}$ with an average of 385 kg $m^{-2}s^{-1}$ [11]. R454C was studied in two papers (223 data points), in two diameters (i.e., 4.7 mm and 5.6 mm), a mass flux range of 80–500 kg $m^{-2}s^{-1}$, and a temperature range of 40–60°C. R455A was studied by two papers (179 data points) and three diameters (i.e., 0.96 mm, 5.6 mm, 8 mm). R455A data have mass fluxes ranging between 80–800 kg $m^{-2}s^{-1}$ and temperatures ranging between 40–45°C . R513A has two papers (58 data points), both of which used multiport extruded tubes with hydraulic diameters around 1 mm. The two papers present three diameters between 0.72–1.16 mm. R513A data had mass flux data ranges from 296–500 kg $m^{-2}s^{-1}$ with an average of 439 kg $m^{-2}s^{-1}$. and temperatures between 40–60°C and an average of 45.7°C [15, 52].

Table 2 Experimental, in-tube flow condensation heat transfer data for synthetic refrigerants

Author	Refrigerants Tested	ID (# of tubes) [mm]	L (mm)	Geometry (shape, roughness, material)	Flow Direction	Tsat (°C)	G (kg $m^{-2}s^{-1}$)	x	Correlations
Agarwal and Hrnjak [53]	R134a, R1234ze(E), R32	6.1	150	Circular, smooth, copper	Horizontal	30–50	100–300	0.05–1	Cavallini et al. [40], Thome et al. [54], Jung et al. [45], Dobson and Chato [37], and Haraguchi et al. [36]
Azzolin et al. [11]	R455A, R452B, R1234yf, R32	0.96/ 8	230/ 1,000	Circular	Horizontal	40	200–400	0–1	Del Col et al. [55]
Del Col et al. [12]	R134a, R1234yf	0.96	230	Circular, copper	Horizontal	40	200–1,000	0.05–0.9	Cavallini et al. [40]
Del Col et al. [42]	R134a, R32	1.23	224	Square, smooth, copper	0/ 15–90° up/down	40	100–390	0.2–0.9	Del Col et al. [42]
Del Col et al. [13]	R1234ze(E)	0.96	230	Circular, smooth, copper	Horizontal	40	100–800	0–0.9	Cavallini et al. [40]

Author	Refrigerants Tested	ID (# of tubes) [mm]	L (mm)	Geometry (shape, roughness, material)	Flow Direction	Tsat (°C)	G (kg $m^{-2}s^{-1}$)	x	Correlations
Del Col et al. [20]	R1234ze(E), R32, R1234ze(E)/ R32 (23/77, 46/54)	0.96	230	Circular, copper	Horizontal	40	200–800	0–1	Cavallini et al. [40]
Diani et al. [19]	R1234yf	3.4	N/A	Circular, microfin	Horizontal	30/ 40	100–1,000	0.2–0.95	Cavallini et al. [56]
Diani et al. [18]	R134a, R1234yf, R1234ze(E)	2.4	N/A	Circular, microfin	Horizontal	30/ 40	300–1,000	0.2–0.95	Cavallini et al. [56], Kedzierski and Goncalves [57]
Diani and Rossetto [58]	R1234yf	3.4	N/A	Circular, microfin	Horizontal	30/ 40	100–800	0.1–1	N/A
Guo et al. [43]	R22, R410A, R32	11.43/ 11.43/ 11.5	2,000	Circular; smooth, herringbone, EHT	Horizontal	47	57–181	0.2–0.8	Shah [34], Cavallini et al. [40]
Guo et al. [24]	R134a, R32, 1234ze(E), R290, R161, R41	2	1,440	Circular, smooth	Horizontal	35–45	200–400	0–1	Baird et al. [59], Garimella et al. [60], Wang et al. [38], Koyama et al. [39], Moser et al. [61], Bandhauer et al. [62], Cavallini et al. [63]
Hirose et al. [44]	R32, R152a, R410A	3.48	660	Circular; smooth, microfin; copper	Horizontal	35	100–400	0.1–0.9	Haraguchi et al. [36], Dobson and Chato [37], Cavallini et al. [40]
Hossain et al. [21]	R410A, R1234ze(E), R32	4.35	3,600	Circular, smooth, copper	Horizontal	35–45	145–400	0.0072–0.999	Cavallini et al. [64, 65], Thome et al. [54], Dobson and Chato [37], Jung et al. [45], Haraguchi et al. [36]
Jacob et al. [51]	R134a, R450A	4.7	1,330	Circular, copper	Horizontal	45/ 55	200–550	0–1	Shah [34], Dobson and Chato [37], Cavallini et al. [40]
Jacob and Fronk [66]	R454C	4.7	1,330	Circular, copper	Horizontal	40–60	100–500	0–1	Shah [34], Dobson and Chato [37], Thome et al. [54], Del Col et al. [55], Cavallini et al. [40], Shah [67], Garimella et al. [60]
Jige et al. [25]	R134a, R32, R1234ze(E), R410A	0.85 (17)	600	MPE rectangular, aluminum alloy	Horizontal	40/ 60	100–400	0–1	Jige et al. [25], Haraguchi et al. [36], Dobson and Chato [37], Cavallini et al. [40], Shah [68]

Author	Refrigerants Tested	ID (# of tubes) [mm]	L (mm)	Geometry (shape, roughness, material)	Flow Direction	Tsat (°C)	G (kg $m^{-2}s^{-1}$)	x	Correlations
Jung et al. [45]	R12, R22, R32, R123, R125, R134a, and R142b	9.52 OD	1,000	Circular, smooth, copper	Horizontal	40	100–300	0.2–1	Traviss et al. [69], Cavallini and Zecchin (1974), Shah [34], Dobson and Chato [37], Akers and Rosson [70], Soliman et al. [71], Tandon et al. [72], Jung et al. [45]
Kim and Kim [73]	R404A, R448A, R449A, R454C, R455A	5.6, 6.44	1,000	Circular; smooth, microfin; copper	Horizontal	45	80–400	0.2–0.9	Yu and Koyama [74], Kedzierski and Goncalves [57], Shikazono et al. [75], Tang et al. [76], Chamra et al. [77], Han and Lee [78], Cavallini et al. [56], Mehendale [79]
Kondou et al. [31]	R134a, R1234ze(E), R1234ze(Z)	5.35	828	Circular, microfin	Horizontal	65	150–400	0–0.9	Kedzierski and Goncalves [57], Chamra et al. [77], Yonemoto and Koyama [80], Cavallini et al. [40]
Kondou et al. [30]	R32/R1234ze(E) (30/70, 40/60), R744/R32/R1234ze(E) (4/43/53, 9/29/62)	5.35	828	Circular, microfin	Horizontal	40	200	0.1–0.9	Kedzierski and Goncalves [57], Chamra et al. [77], Yonemoto and Koyama [80], Cavallini et al. [56]
Kondou et al. [29]	R32/R1234ze(E) (30/70, 40/60), R744/R32/R1234ze(E) (4/43/53, 9/29/62)	5.35	828	Circular, microfin	Horizontal	40	150–400	0.1–0.9	Kedzierski and Goncalves [57], Chamra et al. [77], Yonemoto and Koyama [80], Cavallini et al. [56] with Silver [81] and Bell and Ghaly [82], Chamara and Mago [77]
Kukulka et al. [46]	R22, R410A, R32	11.43/ 11.5	2,000	Circular; smooth, 1EHT; copper	Horizontal	47	57–181	0.2–0.8	N/A
Li et al. [22]	R447A, R32, R134a, R1234ze(E), R410A, R32/R134a mixes, R32/R1234ze(E) mixes	0.86 (15)	480	MPE circular	Horizontal	35/ 40/ 45	100–300	0.05 – 0.96	Thome et al. [54] (2003), Cavallini et al. [83], Shah [84], Wang et al. [38], Park et al. [41], Kim and Mudawar [35]

Author	Refrigerants Tested	ID (# of tubes) [mm]	L (mm)	Geometry (shape, roughness, material)	Flow Direction	Tsat (°C)	G (kg $m^{-2}s^{-1}$)	x	Correlations
Liu et al. [50]	R152a	1.152/ 0.952	336/ 352	Circular, square; stainless steel	Horizontal	40/ 50	200–800	0.1–0.9	Wang et al. [38], Koyama et al. [39], Cavallini et al. [85], Bandhauer et al. [62], Wang and Rose [86]
Liu and Li [47]	R32, R152a, R22	1.152/ 0.952/ 1.304	278/ 288/ 293	Circular, square; stainless steel	Horizontal	30–50	200–800	0.1–0.9	Akers et al. [87], Shah [34], Wang et al. [38], Koyama et al. [39], Cavallini et al. [40]
Liu et al. [26]	R22, R290, R1234ze(E)	1.085/ 0.952	330/ 305	Circular, square; smooth; stainless steel	Horizontal	40/ 50	200–800	0.1–0.9	Kim and Mudawar [35], Wang et al. [38], Koyama et al. [35], Shah [34]
Longo et al. [48]	R410A, R32	4	800	Circular, smooth	Horizontal	29.9 – 40.1	99.3–810.3	0.15 – 0.95	Akers et al. [87], Cavallini and Zecchin [88], Dobson and Chato [37], Wang et al. [38], Koyama et al. [35], Cavallini et al. [40], Kim and Mudawar [35]
Longo et al. [14]	R134a, R152a, R1234yf, R1234ze(E)	4	N/A	Circular, smooth	Horizontal	29.9 – 40.2	75–600	0.13 – 0.96	Akers et al. [87], Cavallini and Zecchin [88], Dobson and Chato [37], Wang et al. [38], Koyama et al. [35], Cavallini et al. [56], Kim and Mudawar [35], Macdonald and Garimella [89]
Lopez-Belchi [15]	R134a, R1234yf, R513A	1.16 (10)/ 0.71 (19)	306	MPE square, triangular; aluminum	Horizontal	30–60	350–940	0.11 – 0.90	Kim et al. [90]
Matkovic et al. [49]	R134a, R32	0.96	230	Circular, smooth, copper	Horizontal	40	100–1,200	0–1	Moser et al. [61], Zhang and Webb [91], Koyama et al. [35] Cavallini et al. [56]
Miyara et al. [23]	R1234ze(E), R32, R410A, R1234ze(E)/ R32 (55/45, 70/30)	4.35	3,600	Circular, smooth, copper	Horizontal	35–45	49–445	0–1	Haraguchi et al. [36], Dobson and Chato [37], Jung et al. [45], Thome et al. [54]
Morrow et al. [52]	R134a, R513A	0.72 (9)	266	MPE, smooth, aluminum	Horizontal	36–40	300/ 400/ 500	0.1–0.8	Kim and Mudawar [35], Shah [84]

Author	Refrigerants Tested	ID (# of tubes) [mm]	L (mm)	Geometry (shape, roughness, material)	Flow Direction	Tsat (°C)	G (kg $m^{-2}s^{-1}$)	x	Correlations
Park et al. [41]	R1234ze(E), R134a, R236fa	1.45 (7)	260	Rectangular, aluminum	Vertical	25–70	50–260	0–1	Bandhauer et al. [62], Cavallini et al. [40], Moser et al. [61], Koyama et al. [39], Thome et al. [54]
Rossato et al. [27]	R32, R1234ze(E)	1.6 (36)	500	MPE rectangular, aluminum	Horizontal	40	55–275	0.1–1	Soliman [71], Traviss et al. [69], Cavallini and Zecchin [88], Shah [34], Dobson and Chato [37], Moser et al. [61], Cavallini et al. [40], Shah [84], Shah [68], Wang et al. [38], Koyama et al. [39], Shah [67], Jige et al. [25]
Toninelli et al. [28]	R134a, R1234ze(E), R32, R717, R290, R152a	0.96/ 1.23/ 1	30–270	Circular, square; smooth	Horizontal	40	65–400	0.1–0.9	Cavallini et al. [40]
Wang et al. [16]	R1234yf, R134a, R32	4	2,250	Circular, smooth, copper	Horizontal	40/ 45/ 50	100–400	0.1–0.9	Shah [34], Cavallini et al. [40], Dobson and Chato [37], Haraguchi et al. [36]
Yang and Nalbandian [17]	R134a, R1234yf	4	600	Circular, smooth, copper	Horizontal	15	200–1,200	0.09–0.9	Shah [34], Cavallini et al. [40], Dobson and Chato [37]

3.2 Natural refrigerants

Research papers which included experimental data has been compiled in Table 3 and include author(s), year published, refrigerants tested, inner tube diameters, test section length, geometry/enhancement, flow direction, saturation temperature, flow rate, quality range, and correlations the results were compared to in the original paper. The most important take away from Table 3 is the relative lack of entries compared to the synthetic table. Although there is an increased emphasis on reducing humanity's global warming footprint in the Paris climate agreement and European F-gas regulations [5], there is less research being conducted investigating flow

condensation with natural refrigerants in small diameter tubes. Natural refrigerants boast very low GWPs, but have tradeoffs, such as the toxicity of ammonia, flammability of propane and R600a, and high pressure required for CO_2. For consumer safety, it is necessary to minimize the charge in air conditioning, heat pumps, and refrigeration systems. Although there are some gaps in data for small diameter in-tube condensation, there are several papers which include natural refrigerants being used in shell and tube heat exchangers with enhanced on-tube condensation [92-95], though that is outside the scope of this paper.

Ammonia (NH_3/R717) data includes a range of diameters (i.e., 1.435 mm – 8.1 mm), mass fluxes (i.e., 20 kg $m^{-2}s^{-1}$ – 270 kg $m^{-2}s^{-1}$), and saturation temperatures (i.e., 24 °C – 60 °C) [Table 3] [96-98]. The average saturation temperature and flow rate for the ammonia data are 37.4 °C and 100 kg/m^2s respectively. This is in stark contrast to the Carbon Dioxide (CO_2/R744) data which has a diameter range with smaller diameters (i.e., 0.1 mm – 6.52 mm), larger mass flux range (i.e., 50 kg $m^{-2}s^{-1}$ – 1,000 kg $m^{-2}s^{-1}$) with an average of 565 kg $m^{-2}s^{-1}$, and wider saturation temperature range (i.e., -25 °C – 30 °C) with an average of 3.5 °C [99-105]. A review of CO_2 compared predictive models, two of which [83, 84] are studied in this paper. Propane (R290) data has a saturation temperature range (40 °C – 50 °C) comparable to ammonia with an average of 40.4 °C as ammonia, but a higher mass flow rate range (35.5 kg $m^{-2}s^{-1}$ – 800 kg $m^{-2}s^{-1}$) with an average of 334 kg $m^{-2}s^{-1}$. It also has a larger diameter range (0.96 mm – 10.07 mm) compared to ammonia yet has a smaller average diameter of 2.74 mm [26, 106-111]. Isobutane (R600a) has similar ranges and averages compared to ammonia with the diameter range being (5.8 mm – 10.07 mm) and average being 7.97 mm. The saturation temperatures tested were all 40 °C and the mass flow rates ranged from (35.5 kg $m^{-2}s^{-1}$ – 300 kg $m^{-2}s^{-1}$) with an average of 94 kg $m^{-2}s^{-1}$ [110-113]. Miyara et

al. [114] reviewed the hydrocarbon research in horizontal tubes, vertical tubes, and plate heat exchangers.

Table 3 Experimental, in-tube flow condensation heat transfer data for natural refrigerants

Author	Refrigerants Tested	ID (# of tubes) [mm]	L (mm)	Geometry (shape, roughness, material)	Flow Direction	Tsat (°C) [Psat (kPa)]	G (kg $m^{-2}s^{-1}$)	x	Correlations
Fronk and Garimella [96]	Ammonia (R717)	1.435	380	Tube	Horizontal	30–60	75,150	0–1	Shah [34], Dobson and Chato [37], Cavallini et al. [64], Bandhauer et al. [62]
Komandiwirya et al. [97]	Ammonia	8.1	914.4	Tube, Finned	Horizontal	24–45	20–270	0–0.95	Thome et al. [54], Cavallini et al. [64]
Vollrath et al. [98]	Ammonia	7.52	914.4	Tube, Finned	Horizontal	40–53	20–270	0–0.95	Cavallini et al. [64], Dobson [115], Thome et al. [54] Chen [116], Shah [34], Tang [117], and Traviss et al. [69]
Fronk and Garimella [99]	CO_2 (R744)	0.1–0.16 (15–40)	51	Rectangular	Horizontal	15/ 20/ 25	400/600/800	0–1	Traviss et al. [69], Shah [34], Dobson and Chato [37], Cavallini et al. [64], Wang et al. [38], Koyama et al. [39], Cavallini et al. [63], Agarwal et al. [118]
Heo et al. [100]	CO_2	0.68 – 1.5 (7–23)	450	Rectangular	Horizontal	(-5)–5	400–800	0–1	Thome et al. [54], Cavallini et al. [64], Bandhauer et al. [62]
Iqbal and Bansal [101]	CO_2	6.52	500	Circular, Smooth	Horizontal	(-15) –0	50 – 200	0–1	Akers et al. [87], Dobson and Chato [37], Shah [34], Li et al. [119], Tandon et al. [72]
Kang et al. [102]	CO_2	5.15	2,200	Circular, Smooth	Horizontal	(-10) –5	600 – 1,000	0–1	Shah [34], Cavallini and Zecchin [88], Thome et al. [54]
Kim et al. [103]	CO_2	3.48/ 3.51	250	Circular, Smooth,Fin	Horizontal	(-25) – (-15)	200 – 800	0–1	Bivens and Yokozeki [120], Dobson and Chato [37], Cavallini et al. [64], Thome et al. [54]

Author	Refrigerants Tested	ID (# of tubes) [mm]	L (mm)	Geometry (shape, roughness, material)	Flow Direction	Tsat (°C) [Psat (kPa)]	G (kg $m^{-2}s^{-1}$)	x	Correlations
Park and Hrnjak [105]	CO_2	0.89	500	Circular,Smooth	Horizontal	(-25) – (-15)	200 – 800	0–1	Koyama et al.[39], Dobson and Chato [37], Cavallini et al. [65], Thome et al. [54], Jaster and Kosky [121], Akers et al. [87], Soliman et al. [71], Traviss et al. [69], Shah [34], Chen et al. [122]
Son and Oh [104]	CO_2	4.95	2,400	Circular, Smooth	Horizontal	20 –30	400 – 800	0.1 – 0.9	Cavallini and Zecchin [88], Dobson and Chato [37], Shah [34], Cavallini et al. [40], Kondou and Hrnjak [123]
Son and Oh [104]	CO_2	4.6	2,400	Circular,Fin	Horizontal	20 –30	400 – 800	0.1 –1	Han and Lee [78], Chamra et al. [77], Haraguchi et al. [36], Cavallini et al. [56], Koyama and Yonemoto [80], Kedzierski and Goncalves [57], Koyama et al. [39]
Ghorbani et al. [113]	R600a	8.7	1,050	Flat	Horizontal	36.2 – 45.6	110– 372	.01 – 0.85	Traviss et al. [69], Cavallini and Zecchin [88], Dobson [115], Shah [84] Jung et al. [45]
Agra and Teke [112]	R600a	4	N/A	Circular	Horizontal	30–43	50–100	0.5 –1	N/A
Del Col et al. [108]	Propane (R290)	0.96	N/A	Round	Horizontal	40	100– 800	0– 0.9	Matkovic et al. [49], Cavallini et al. [40]
Del Col et al. [107]	Propane	0.96	228	Circular	Horizontal	40	200– 800	0.5 –1	Cavallini et al. [40]
Fernando et al. [109]	Propane	1.42 (6)	661	Rectangular	Vertical	30/ 40/ 50	20–50	N/A	Nusselt [124], Dobson and Chato [37], Di-an and Yongren [125], Kutateldze [126], Chato [127], Shah [34], Akers [70], Tandon et al. [72], Shao [128], Chen [122]

Author	Refrigerants Tested	ID (# of tubes) [mm]	L (mm)	Geometry (shape, roughness, material)	Flow Direction	Tsat (°C) [Psat (kPa)]	G (kg $m^{-2}s^{-1}$)	x	Correlations
Lee and Son [110]	R600a, Propane	10.07/ 7.73/ 6.54/ 5.8	5,000	Round	Horizontal	40	35.5–210.4	0–0.9	Shah [34], Traviss et al. [69], Cavallini and Zecchin [88], Haraguchi et al. [36], Dobson et al. [129]
Liu et al. [26]	Propane	1.085/ 0.952	420/ 400	Round,Square	Horizontal	40–50	200–800	0.1–0.9	Kim and Mudawar [35], Wang et al. [38], Koyama et al. [35], Shah [34]
Park et al. [111]	Propane, R600a	8.8	530	Round	Horizontal	40	100/ 200/ 300	0.1–0.9	Akers et al. [87], Cavallini and Zecchin [88], Dobson and Chato [37], Jung et al. [45], Shah [34], Soliman et al. [71], Traviss et al. [69]

4. Predicted condensation heat transfer for low GWP alternatives

4.1 Condensation correlations studied

Heat transfer data were extracted from the literature for synthetic refrigerant flow condensation in smooth (i.e., 4,098 data points from 33 papers) and microfin tubes (i.e., 591 data points from 7 papers) as well as flow condensation of natural refrigerants in smooth (i.e., 1,413 data points from 18 papers) and microfin tubes (i.e., 60 data points from 2 papers). The experimental heat transfer coefficients were extracted using graph extraction software (Web Plot Digitizer) and exported into an Excel file that kept track of first author, year, refrigerant, diameter, mass flux, quality, saturation temperature, and heat transfer coefficients of each data point. These heat transfer coefficients were compared to correlations selected from the correlations used in the reviewed papers, as shown in Table 2 and Table 3. Smooth tube correlations analyzed in this paper include Akers et al. [87], Cavallini et al. [83], Cavallini et al. [85], Kim and Mudawar [35], Macdonald and Garimella [89], Shah [34], Shah [84], Shah [68], Shah [67], and Traviss et al. [69] and enhanced tube correlations developed by Chamra et al. [77] and Kedzierski and Goncalves

[57], as summarized in Table 4. Most of the correlations used in this paper were used by at least two of the reviewed papers.

The correlations selected for further analysis do not depend on the fluid temperature-wall temperature difference – either directly or in the Jakob number (Ja) – as wall temperatures were rarely accessible in the extracted data [11], and wall temperatures are not always known for design problems. These fluid – wall temperature differences are required for many popular flow condensation correlations, including Bandhauer et al. [62], Cavallini et al. [65], Cavallini et al. [40], Dobson and Chato [37], Jige et al. [25], Jung et al. [45], Koyama et al. [39], Moser et al. [61], Park et al. [41], Soliman et al. [71], Thome et al. [54], Wang et al. [38], Wang and Rose [86], Cavallini et al. [56], Kedzierski and Kim [130], etc. Compared to boiling in which the fluid-wall temperature difference is critical for bubble formation [131], for condensation, the fluid-wall temperature difference has lesser effects on the heat transfer coefficients particularly in flow condensation [132]. The refrigerants that were compared to the correlations were refrigerants with an ASHRAE designation. Self-made refrigerant mixtures without ASHRAE designations presented in papers were not compared due to the uncertainties in calculating refrigerant properties.

Table 4 Summary of condensation correlations

Name	Correlation equations	Experimental conditions and test samples	Uncertainties presented
Akers et al. (1959) [87]	If Re_E<5E4 $Nu_l = 5.03 Re_E^{1/3} Pr_l^{1/3}$ If Re_E>5E4 $Nu = 0.0265 Re_E^{0.8} Re^{0.8} Pr_l^{1/3}$ Where $Re_E = \frac{D G_E}{\mu_l}$ $G_E = G_l + G_v \left(\frac{\rho_l}{\rho_v}\right)^{1/2}$	Propane and R12; D=15.8 mm; ρ_v=57.7 – 352 kg m^{-3}; ρ_l=256 – 1,153 kg m^{-3}; μ_l=34.97e-6 – 227.4e-6 kg m^{-1}s^{-1}; c_{pl}=2.97 – 33.5 kJ kg^{-1}K^{-1}; k_l=57.98 – 74.42 mW m^{-1}K^{-1}; heat of vaporization 40.94 – 241.9 kJ kg^{-1}	N/A

Name	Correlation equations	Experimental conditions and test samples	Uncertainties presented
Cavallini et al. (2006) [83]	$$h = \frac{\rho_l c_{p_l} \left(\frac{\tau_i}{\rho_l}\right)^{0.5}}{T^+}$$ $$\tau_i = \frac{\left(dp/dz\right)_f D_h}{4}$$ If $\delta^+ \leq 5$, $$T^+ = \delta^+ Pr_l$$ If $5 < \delta^+ \leq 30$, $$T^+ = 5\left\{Pr_l + ln\left[1 + Pr_l\left(\frac{\delta^+}{5} - 1\right)\right]\right\}$$ If $\delta^+ \geq 30$, $$T^+ = 5\{Pr_l + ln(1 + 5Pr_l) + 0.495\}$$ And if $Re_{lf} \leq 1145$, $$\delta^+ = \left(\frac{Re_{lf}}{2}\right)^{1/2}$$ Else if $Re_{lf} \geq 1145$, $$\delta^+ = 0.0504 Re_{lf}^{7/8}$$ Where $$Re_{lf} = \frac{G(1-x)(1-E)D}{\mu_l}$$	R11, R12, R123, R134a, R22, R236ea, R404A, R407C, R410A; D=0.691–7.79mm; G=70–1,400 kg m^{-2}s^{-1}	N/A
Cavallini et al. (2011) [85]	$$h = h_{LO}\left[1 + 1.128x^{0.8170}\left(\frac{\rho_l}{\rho_v}\right)^{0.3685}\left(\frac{\mu_l}{\mu_v}\right)^{0.2363}\left(1 - \frac{\mu_v}{\mu_l}\right)^{2.144} Pr_l^{-0.100}\right]$$ $$h_{lo} = 0.023 Re_{lo}^{0.8} Pr_l^{0.4} \frac{k_l}{D}$$ $$Re_{lo} = \frac{GD}{\mu_l}$$	R245fa, R32; D=0.96 mm; G=100–1,200 kg m^{-2}s^{-1} (mass fluxes above 200 kg m^{-2}s^{-1} predicted using annual flow models)	N/A

Name	Correlation equations	Experimental conditions and test samples	Uncertainties presented
Chamra et al. (2005) [77]	$$h = \frac{A_1 \rho_l c_{pl} (\tau_w/\rho_l)^{A_2}}{T^+} Rx^{A_3}$$ where A_1, A_2, and A_3 are empirical values corresponding to 0.208, 0.224, and 1.321, respectively, τ_w is wall shear stress, Rx is an empirically fitted relative roughnees for microfins, $$Rx = \frac{0.18(e/d)}{(0.1 + cos\beta)}$$ where e is microfin height and β is microfin apex angle. T^+ is nondimensional temperatura, defined as, $$T^+ = \delta^+ Pr_l, \delta \leq 5$$ $$T^+ = 5\left[Pr_l + ln\left[1 + Pr_l\left(\frac{\delta^+}{5} - 1\right)\right]\right], 5 < \delta^+ \leq 30$$ $$T^+ = 5\left[Pr_l + ln(1 + 5Pr_l) + 0.5ln\left(\frac{\delta^+ - 2.5}{27.5}\right)\right], \delta^+ > 30$$ Where $$\delta^+ = 0.866 Re_{ls}^{0.5}, Re_{ls} \leq 1600$$ $$\delta^+ = 0.051 Re_{ls}^{0.87}, Re_{ls} > 1600$$ $$Re_{ls} = \frac{G(1-x)D}{\mu_l}$$	R134a, R22; G=40–850 kg m^{-2}s^{-1}; D=6.7–15.38 mm; Microfin data	MAE=20%
Kedzierski and Goncalves (1999) [57]	$$h = 4.94 Re_{lo}^{0.235} Pr_l^{0.308} \left(\frac{p}{p_c}\right)^{-1.16x^2} \left(-log_{10}\frac{p}{p_c}\right)^{-0.887x^2} Sv^{2.708x} \frac{k_l}{D}$$ where $$Sv = \frac{(v_v - v_l)}{x v_v + (1-x) v_l}$$ $$Re_{lo} = \frac{GD}{\mu_L}$$	R125, R134a, R32 R410A; D=9.5 mm; G=57-522 kg m^{-2}s^{-1}; Nu=58 – 508; Re=3,500 – 24,000; Ja=6 – 256; Pr=1.7 – 3.6; P_r=0.22 – 0.62; Sv=0.86 – 10.3	MAE=23.5%

Name	Correlation equations	Experimental conditions and test samples	Uncertainties presented
Kim and Mudawar (2013) [35]	For annular flows, determined by $We^* > 7{X_{tt}}^{0.2}$ $$Nu_l = 0.048{Re_l}^{0.69}{Pr_l}^{0.34}\frac{\varphi_v}{X_{tt}}$$ For non-annular flows, $We^* < 7{X_{tt}}^{0.2}$ $$Nu_l = \left[\left(0.048{Re_l}^{0.69}{Pr_l}^{0.34}\frac{\varphi_v}{X_{tt}}\right)^2 + \left(3.2*10^{-7}{Re_l}^{-0.38}{Su_{vo}}^{1.39}\right)^2\right]^{0.5}$$ Criterion includes the modified Weber number, We^*, defined as For $Re_l \le 1250$ $$We^* = 2.45\frac{{Re_v}^{0.64}}{{Su_{vo}}^{0.3}\left(1+1.09{X_{tt}}^{0.039}\right)^{0.4}}$$ For $Re_l > 1250$ $$We^* = 0.85\frac{{Re_v}^{0.79}{X_{tt}}^{0.157}}{{Su_{vo}}^{0.3}\left(1+1.09{X_{tt}}^{0.039}\right)^{0.4}}\left[\left(\frac{\mu_v}{\mu_l}\right)^2\left(\frac{\rho_l}{\rho_v}\right)\right]^{0.084}$$ Where $$X_{tt} = \left(\frac{\mu_l}{\mu_v}\right)^{0.1}\left(\frac{1-x}{x}\right)^{0.9}\left(\frac{\rho_v}{\rho_l}\right)^{0.5}$$ $${\varphi_g}^2 = 1 + CX + X^2$$ $$X^2 = \frac{(dP/dz)_l}{(dP/dz)_v}$$ $$-\left(\frac{dP}{dz}\right)_f = \frac{2f_f v_f G^2(1-x)^2}{D_h}$$ $$-\left(\frac{dP}{dz}\right)_g = \frac{2f_g v_g G^2 x^2}{D_h}$$ $$Su_{vo} = \frac{\rho_v \sigma D_h}{\mu_l^2}$$	R12, R123, R1234yf, R1234ze(E), R134a, R22, R236fa, R245fa, R32, R404A, R410A, R600a, FC72, methane, CO_2; D= 0.424–6.22 mm; G= 53-1403 kg $m^{-2}s^{-1}$; Re_{lo}=276 – 89,798; P_r=0.04 – 0.91	MAE=16%

Name	Correlation equations	Experimental conditions and test samples	Uncertainties presented
Macdonald and Garimella (2016) [89]	$$h_{condensation} = \frac{h_{film}\theta + h_{pool}(2\pi - \theta)}{2\pi}$$ $$h_{upper\ film} = A \cdot h_{ff} + B \cdot h_{annular}$$ With different parameters (e.g., δ, ε, etc.) based on stratified ($Fr \leq 7$) or annular ($Fr > 7$) flow regimes, where $$Fr = 1.26 Re_{ls}^{1.04} Ga^{-0.5} (1 + 1.09 X_{tt}^{0.039})^{1.5} X_{tt}^{-1.5}$$ and $$Re_{ls} = \frac{G(1-x)D}{\mu_l}$$ $$Ga = \frac{gD^3\rho_l^2}{\mu_l^2}$$ $$h_{annular} = \frac{0.0039 Re_{ulf}^{0.775} Pr_l^{0.3} \kappa_i \kappa_E k_l}{\delta_{lf}}$$ $$h_{ff} = \frac{0.2 Re_{ulf}^{-0.08} \kappa_i k_l}{l_{ff}} \text{ and } l_{ff} = \left[\frac{(\mu_l/\rho_l)^2}{g}\right]^{1/3}$$ $$h_{pool} = \frac{0.023 Re_{ls}^{0.8} Pr_l^{0.3} k_l}{D}$$ $$Re_{ulf} = \frac{4G(1-x)\delta_f}{(1-\varepsilon)\mu_l}\xi$$ $$Re_{ls} = \frac{G(1-x)D}{\mu_l}$$	CO_2, ethane, pentane, propane, R245fa, R404A, R410A; D=7.75–14.45 mm; G=150–450 kg m^{-2}s^{-1}; P_r=0.25 – 0.94	MAE=12%
Shah (1979) [34]	$$h_{lo} = 0.023 {Re_{lo}}^{0.8} {Pr_l}^{0.4} \frac{k_l}{D}$$ $$h = h_{lo}\left[(1-x)^{0.8} + \frac{3.8x^{0.76}(1-x)^{0.04}}{{p_r}^{0.38}}\right]$$ where $$Re_{lo} = \frac{GD}{\mu_L}$$	Water, R11, R12, R22, R113, methanol, ethanol, benzene, toluene, trichloroethylene; D=7–40 mm; G 10.83–210.6 kg m^{-2}s^{-1}; P_r=0.002 – 0.44; Re_{lo}=100 – 63,000; Pr_l=1 – 13	MAE=15.4%

Name	Correlation equations	Experimental conditions and test samples	Uncertainties presented
Shah (2009) [84]	Regime I ($j_v \geq \frac{1}{2.4Z+0.73}$): $$h = h_1$$ Regime II ($j_v \leq 0.89 - 0.93e^{(-0.087Z^{-1.17})}$): $$h = h_1 + h_2$$ Regime III ($j_v \geq 0.89 - 0.93e^{(-0.087Z^{-1.17})}$): $$h = h_2$$ where $$h_1 = h_{ls}\left(\frac{\mu_l}{14\mu_v}\right)^n \left[(1-x)^{0.8} + \frac{3.8x^{0.76}(1-x)^{0.04}}{{p_r}^{0.38}}\right]$$ $$n = 0.0058 + 0.557p_r$$ $$h_{ls} = 0.023Re_{lo}^{0.8}Pr_l^{0.4}$$ $$h_2 = 1.32{Re_{ls}}^{-1/3}\left[\frac{\rho_l(\rho_l-\rho_v)g{k_l}^3}{{\mu_l}^2}\right]^{1/3}$$ $$Re_{ls} = \frac{G(1-x)D}{\mu_l}$$ $$Z = \left(\frac{1}{x}-1\right)^{0.8} p_r^{0.4}$$ $$j_v = \frac{xG}{[gD\rho_v(\rho_l-\rho_v)]^{0.5}}$$	Benzene, Dowtherm 209, ethanol, isobutane, methanol, propane, propylene, toluene, R11, R113, R12, R123, R125, R134a, R142b, R22, R32, R404A, R410A, R502, R507, water; D= 2–49 mm; G= 4-820 kg m^{-2}s^{-1}; P_r=0.0008 – 0.9; Re_{lo}=68 – 85,000; Pr_l=1 – 18	MAE=14.4%
Shah (2013) [68]	Regime I ($j_v \geq 0.98(Z+0.263)^{-0.62}$): $$h = h_1$$ Regime II occurs when superficial velocities are between Regime I and III boundaries: $$h = h_1 + h_2$$ Regime III ($j_v \leq 0.95(1.254 + 2.27Z^{1.249})^{-1}$): $$h = h_2$$ where $$h_1 = h_{ls}\left(\frac{\mu_l}{14\mu_v}\right)^n \left[(1-x)^{0.8} + \frac{3.8x^{0.76}(1-x)^{0.04}}{{p_r}^{0.38}}\right]$$ $$n = 0.0058 + 0.557p_r$$ $$h_{ls} = 0.023Re_{ls}^{0.8}Pr_l^{0.4}$$ $$h_2 = 1.32{Re_{ls}}^{-1/3}\left[\frac{\rho_l(\rho_l-\rho_g)g{k_l}^3}{{\mu_l}^2}\right]^{1/3}$$ $$Re_{ls} = \frac{G(1-x)D}{\mu_l}$$ $$Z = \left(\frac{1}{x}-1\right)^{0.8} p_r^{0.4}$$ $$j_v = \frac{xG}{[gD\rho_v(\rho_l-\rho_v)]^{0.5}}$$	Benzene, CO_2, dimethyl ether, Dowtherm 209, ethanol, isobutane, methanol, propane, propylene, R11, R12, R22, R32, R113, R123, R125, R134a, R142b, R404A, R410A, R502, R507, toluene, water; D=2–49 mm; G=4–820 kg m^{-2}s^{-1}; P_r=0.0008 – 0.946; Re_{lo}=68 – 84827; Pr_l=1 – 18	MAE=16.1%

Name	Correlation equations	Experimental conditions and test samples	Uncertainties presented
Shah (2016) [67]	Regime I (We_{vo}>100 and $j_v \geq 0.98(Z+0.263)^{-0.62}$): $h = h_1$ Regime II (We_{vo}<100 and $j_v \geq 0.98(Z+0.263)^{-0.62}$): $h = h_1 + h_2$ Regime III ($j_v \leq 0.95(1.254+2.27Z^{1.249})^{-1}$): $h = h_2$ where $We_{vo} = \frac{G^2 D}{\rho_v \sigma}$ $h_1 = h_{lo}\left[1 + 1.128x^{0.817}\left(\frac{\rho_l}{\rho_v}\right)^{0.3685}\left(\frac{\mu_l}{\mu_v}\right)^{0.2363}\left(1 - \frac{\mu_v}{\mu_l}\right)^{2.144} {Pr_l}^{-0.1}\right]$ $h_2 = 1.32 {Re_{ls}}^{-1/3}\left[\frac{\rho_l(\rho_l-\rho_v)g{k_l}^3}{{\mu_l}^2}\right]^{1/3}$ $h_{lo} = 0.023 {Re_{lo}}^{0.8} {Pr_l}^{0.4}\frac{k_l}{D}$ $Re_{lo} = \frac{GD}{\mu_L}$ $Re_{ls} = \frac{G(1-x)D}{\mu_l}$	Butane, CO_2, FC-72, propane, R1234fa, R1234ze(E), R134a, R152a, R22, R245fa, R32, R410A, water; D= 0.1–2.8 mm; G= 20–1400 kg m^{-2}s^{-1}; P_r=0.0055 – 0.942; Re_{lo}=121 – 20367; We_{vo}=5 – 8108; Bond number=0.033 – 29.4	MAE=15.5%
Traviss et al. (1973) [69]	$Nu = F(X_{tt})\frac{Pr_l {Re_{ls}}^{0.9}}{F_2}$ $F(X_{tt}) = 0.15\left[{X_{tt}}^{-1} + 2.85 {X_{tt}}^{-0.476}\right]$ Where $X_{tt} = \left(\frac{\mu_l}{\mu_v}\right)^{0.1}\left(\frac{1-x}{x}\right)^{0.9}\left(\frac{\rho_v}{\rho_l}\right)^{0.5}$ If Re_{ls}< 50, $F_2 = 0.707 Pr_l Re_{ls}^{0.5}$ If 50< Re_{ls}< 1125, $F_2 = 5Pr_l + 5ln[1 + Pr_l(0.09636 Re_{ls}^{0.585} - 1)]$ And if Re_{ls}> 1125, $F_2 = 5Pr_l + 5ln(1+5Pr_l) + 2.5ln(0.00313 Re_l^{0.812})$ $Re_{ls} = \frac{G(1-x)D}{\mu_l}$	R12, R22, D=15.6 mm, G=374–1533 kg m^{-2}s^{-1}	MAE=7%

4.2 Correlation performance for synthetic refrigerants in smooth tubes

Table 5 presents information on the refrigerants that are used in the correlation comparisons. A wide range of synthetic refrigerants were found in literature, including refrigerants with zero Ozone Depletion Potential and GWPs below 700 (e.g., R32, R450A, R452B) and below 150 [e.g., R152a, R161, R1234yf, R1234ze(E), R1234ze(Z), etc.]. It should be noted that of the

synthetic refrigerants, most fluids with GWPs lower than 150 are, at minimum, mildly-to-somewhat flammable and classified as A2Ls or A2s. In the literature, some refrigerants have heat transfer coefficient data covering a wide range of diameters (eg., R134a, R410A, etc.), while others emerging refrigerants have limited flow condensation data (e.g., R41, R161, R513A, etc.).

Table 5 Refrigerant classifications and GWP values, as well as the tube type (S: Smooth, MF: microfin) and inner diameter range (unless otherwise denoted with OD) from extracted data

Refrigerant	Type	ODP	GWP	Safety	Tube type	Diameter range [mm]
R12	CFC	1	10,200	A1	S	9.52 OD – 9.64
R22	HCFC	0.05	1,000	A1	S	0.952 – 11.5
R32	HFC	0	677	A2L	S/MF	0.85 – 11.5
R41	HFC	0	116		S	2
R123	HCFC	0.02	79	B1	S	9.52 OD
R125	HFC	0	3,170	A1	S	9.52 OD
R134a	HFC	0	1,300	A1	S/MF	0.71 – 9.64
R142b	HCFC	0.07	2,310	A2	S	9.52 OD
R152a	HFC	0	138	A2	S/MF	0.952 – 9.64
R161	HFC	0	4		S	2
R404A	HFC	0	3,922		S/MF	5.6 – 6.44
R410A	HFC	0	2,088	A1	S/MF	0.85 – 11.5
R447A	HFC/HFO		572		S	0.86
R448A	HFC/HFO	0	1273	A1	S/MF	5.6 – 6.44
R449A	HFC/HFO	0	1282	A1	S/MF	5.6 – 6.44
R450A	HFC/HFO		604	A1	S	4.7
R452B	HFC/HFO	0	675	A2L	S	0.96 – 8
R454C	HFC/HFO	0	148	A2L	S/MF	5.6 – 6.44
R455A	HFC/HFO	0	146	A2L	S/MF	0.96 – 8
R513A	HFC/HFO	0	573	A1	S	0.71 – 1.16
R1234yf	HFO	0	4	A2L	S/MF	0.71 – 8
R1234ze(E)	HFO	0	<1	A2L	S/MF	0.85 – 6.1
R1234ze(Z)	HFO	0	<1	A2L	MF	5.35

The predicted heat transfer coefficients were plotted against the experimental heat transfer coefficients for each correlations. These plots are included Appendix A for the synthetic refrigerants and Appendix B for the natural refrigerants. Figure A.1 presents the smooth tube

correlation predictions using synthetic refrigerants; mean average error (MAE) values are presented in Table 6 and are color coded: green (MAE ≤ 20%), yellow (20%<MAE<50%), and red (MAE ≥ 50%). The MAE is calculated as follows:

$$MAE = average\left(abs\left(\frac{h_{pred} - h_{exp}}{h_{exp}}\right)\right) \quad (1)$$

The correlations were analyzed by refrigerant, diameter, mass flux, quality, and liquid-only Reynolds number. The analysis showed that diameter and mass flux had the strongest impact on MAE of the correlations. There were no discernable patterns for prediction performance based on quality or Reynolds number. For diameter, the diameter range the correlation was developed for greatly influenced how well the correlation predicted a given diameter range. For example, Akers et al. [87] struggled with tube diameters less than 4 mm. One interesting note, the Kim and Mudawar [35] and Shah [67, 68, 84] correlations had larger MAEs for the 3 – 4 mm range compared to diameters both above and below. Because of flow regime changes moving from macro- to micro-scale tubes, this could be due to the transition between the two scales; however, there was only one paper in the 3 – 4 mm diameter range, so it is hard to draw any conclusions based on the current data. Table 6 presents the MAE for each correlation broken down by refrigerant, then diameter in 1 mm increments, then mass flux in 200 kg $m^{-2}s^{-1}$ increments. The total MAE for each correlation is presented at the bottom of the table. All but two correlations had a total MAE of less than 50%, with Akers et al. [87] being over 100% and was developed for two fluids (i.e., R12 and propane) condensing in a 15.8 mm diameter tube, which is larger than the diameters analyzed in this work. The table also shows that Akers et al. [87] struggles to predict data in tubes small than 5 mm and tends to do better at higher mass fluxes. The Macdonald and Garimella [89] correlation was developed primarily using natural refrigerants which may explain

the discrepancies. There were no other discernable trends as to why it did not predict the refrigerants well. Due to the iterative nature of the correlation, there were data points that were not able to be calculated, including any data in the 11 – 12 mm diameter group. The overall best performing correlation was Kim and Mudawar [35], with the Cavallini et al. [83, 85] and Shah [84] correlations being close behind. For HFO refrigerants, Kim and Mudawar [35] predicts both R1234yf and R1234ze(E) the best, though R1234yf is not well predicted by any correlation. For low GWP HFCs and HFC/HFO mixtures, the Cavallini et al. [83, 85] correlations generally predicted the condensation heat transfer behavior of synthetic refrigerants the best, except for R513A. The data for R513A are limited to two papers with tube diameters at the lower range, 0.72 [52], 0.71, and 1.16 mm [15]. The table shows that the correlations generally predicted the R513A less than 1 mm well and the data greater than 1 mm not well.

Table 6 Mean average error (MAE) predictions of synthetic refrigerant data for smooth tubes broken down by refrigerant, then diameter, then mass flux (*Due to the iterative nature of the correlation, not all data was able to be predicted.)

	# of points	Akers [87]	Cav06* [83]	Cav11 [85]	Kim [35]	Macdonald* [89]	Shah79 [34]	Shah09 [84]	Shah13 [68]	Shah16 [67]	Travis [69]
R1234yf	**307**	**106%**	**41%**	**39%**	**37%**	**55%**	**48%**	**53%**	**45%**	**63%**	**55%**
0-1 mm	**106**	**122%**	**11%**	**7%**	**8%**	**26%**	**20%**	**25%**	**39%**	**35%**	**62%**
200-400 kg $m^{-2}s^{-1}$	35	205%	9%	6%	6%	24%	18%	23%	34%	32%	60%
400-600 kg $m^{-2}s^{-1}$	24	121%	6%	5%	8%	25%	19%	24%	39%	34%	61%
600-800 kg $m^{-2}s^{-1}$	13	82%	8%	7%	10%	27%	20%	26%	40%	37%	62%
800-1000 kg $m^{-2}s^{-1}$	23	57%	15%	8%	8%	29%	22%	28%	43%	39%	63%
1000-1200 kg $m^{-2}s^{-1}$	11	41%	19%	9%	9%	28%	22%	28%	44%	40%	63%
1-2 mm	**44**	**292%**	**128%**	**126%**	**112%**	**182%**	**156%**	**178%**	**39%**	**198%**	**18%**
400-600 kg $m^{-2}s^{-1}$	33	291%	112%	112%	100%	169%	140%	165%	34%	182%	21%
600-800 kg $m^{-2}s^{-1}$	11	295%	177%	169%	147%	221%	205%	219%	56%	247%	9%
4-5 mm	**157**	**44%**	**37%**	**36%**	**36%**	**38%**	**36%**	**37%**	**50%**	**45%**	**62%**
0-200 kg $m^{-2}s^{-1}$	49	49%	41%	40%	40%	38%	34%	34%	54%	39%	67%

200-400 kg $m^{-2}s^{-1}$	57	50%	38%	36%	37%	38%	37%	38%	50%	46%	63%
400-600 kg $m^{-2}s^{-1}$	25	37%	33%	35%	34%	41%	39%	41%	49%	47%	62%
600-800 kg $m^{-2}s^{-1}$	12	26%	51%	47%	31%	69%	63%	69%	38%	90%	46%
800-1000 kg $m^{-2}s^{-1}$	9	37%	10%	13%	28%	7%	6%	6%	53%	8%	69%
1000-1200 kg $m^{-2}s^{-1}$	5	30%	24%	9%	20%	12%	13%	12%	29%	34%	61%
R1234ze(E)	**715**	**108 %**	**31%**	**29%**	**27%**	**30%**	**29%**	**29%**	**43%**	**34%**	**66%**
0-1 mm	**235**	**160 %**	**23%**	**19%**	**18%**	**23%**	**23%**	**24%**	**38%**	**30%**	**64%**
0-200 kg $m^{-2}s^{-1}$	71	224%	22%	28%	20%	22%	25%	25%	28%	23%	71%
200-400 kg $m^{-2}s^{-1}$	65	192%	31%	29%	30%	30%	29%	30%	47%	37%	60%
400-600 kg $m^{-2}s^{-1}$	50	118%	15%	3%	5%	20%	17%	19%	39%	29%	62%
600-800 kg $m^{-2}s^{-1}$	17	80%	18%	7%	11%	20%	17%	19%	42%	30%	62%
800-1000 kg $m^{-2}s^{-1}$	32	60%	22%	8%	12%	22%	19%	21%	42%	33%	62%
1-2 mm	**283**	**100 %**	**32%**	**34%**	**30%**	**31%**	**29%**	**29%**	**42%**	**32%**	**69%**
0-200 kg $m^{-2}s^{-1}$	138	90%	32%	41%	28%	33%	29%	29%	31%	27%	78%
200-400 kg $m^{-2}s^{-1}$	95	128%	45%	35%	42%	38%	37%	38%	56%	43%	61%
400-600 kg $m^{-2}s^{-1}$	44	71%	5%	11%	12%	11%	9%	11%	48%	19%	67%
800-1000 kg $m^{-2}s^{-1}$	6	81%	37%	23%	18%	48%	41%	47%	36%	61%	54%
2-3 mm	**36**	**106 %**	**18%**	**13%**	**11%**	**22%**	**21%**	**22%**	**42%**	**29%**	**63%**
200-400 kg $m^{-2}s^{-1}$	30	107%	16%	12%	10%	20%	19%	20%	43%	26%	64%
400-600 kg $m^{-2}s^{-1}$	6	100%	32%	18%	15%	32%	32%	32%	34%	41%	58%
4-5 mm	**161**	**46%**	**44%**	**39%**	**39%**	**40%**	**40%**	**39%**	**53%**	**43%**	**63%**
0-200 kg $m^{-2}s^{-1}$	29	75%	33%	30%	34%	32%	30%	31%	47%	37%	58%
200-400 kg $m^{-2}s^{-1}$	102	39%	40%	38%	38%	35%	35%	34%	58%	34%	69%
400-600 kg $m^{-2}s^{-1}$	18	49%	63%	49%	47%	58%	58%	58%	47%	69%	53%
600-800 kg $m^{-2}s^{-1}$	12	30%	83%	56%	44%	75%	73%	75%	35%	98%	43%
R134a	**770**	**105 %**	**27%**	**28%**	**26%**	**30%**	**29%**	**30%**	**42%**	**34%**	**66%**
0-1 mm	**250**	**141 %**	**15%**	**16%**	**15%**	**18%**	**18%**	**19%**	**40%**	**23%**	**68%**
0-200 kg $m^{-2}s^{-1}$	60	180%	29%	36%	21%	30%	32%	31%	28%	26%	77%
200-400 kg $m^{-2}s^{-1}$	75	224%	15%	11%	11%	20%	20%	21%	37%	29%	63%
400-600 kg $m^{-2}s^{-1}$	38	144%	12%	9%	6%	21%	20%	21%	33%	30%	61%
600-800 kg $m^{-2}s^{-1}$	11	64%	3%	5%	12%	9%	9%	9%	48%	17%	68%

800-1000 kg m^{-2}s^{-1}	33	33%	5%	6%	13%	7%	6%	7%	55%	14%	71%
1000-1200 kg m^{-2}s^{-1}	33	11%	10%	11%	21%	5%	5%	5%	61%	9%	73%
1-2 mm	**270**	**121 %**	**40%**	**43%**	**38%**	**41%**	**40%**	**40%**	**41%**	**40%**	**67%**
0-200 kg m^{-2}s^{-1}	132	97%	35%	40%	31%	32%	31%	31%	33%	26%	79%
200-400 kg m^{-2}s^{-1}	100	89%	13%	16%	19%	8%	8%	8%	55%	6%	72%
400-600 kg m^{-2}s^{-1}	27	283%	109%	111%	101 %	150%	134%	148%	28%	162%	27%
600-800 kg m^{-2}s^{-1}	11	294%	180%	163%	144 %	194%	190%	194%	50%	219%	11%
2-3 mm	**45**	**81%**	**9%**	**9%**	**10%**	**11%**	**11%**	**11%**	**44%**	**19%**	**66%**
200-400 kg m^{-2}s^{-1}	35	90%	9%	10%	8%	12%	12%	12%	45%	19%	66%
400-600 kg m^{-2}s^{-1}	10	49%	8%	7%	14%	9%	9%	9%	42%	17%	65%
4-5 mm	**186**	**48%**	**30%**	**28%**	**30%**	**35%**	**33%**	**35%**	**43%**	**44%**	**59%**
0-200 kg m^{-2}s^{-1}	33	70%	32%	31%	34%	32%	35%	35%	49%	34%	64%
200-400 kg m^{-2}s^{-1}	60	59%	34%	33%	35%	38%	36%	37%	45%	46%	59%
400-600 kg m^{-2}s^{-1}	62	35%	20%	20%	24%	31%	26%	30%	41%	42%	60%
600-800 kg m^{-2}s^{-1}	18	31%	49%	44%	35%	59%	55%	58%	38%	78%	48%
800-1000 kg m^{-2}s^{-1}	8	28%	24%	9%	18%	5%	6%	5%	44%	17%	65%
1000-1200 kg m^{-2}s^{-1}	5	22%	38%	14%	8%	16%	17%	16%	22%	38%	59%
9-10 mm	**19**	**29%**	**22%**	**24%**	**30%**	**21%**	**10%**	**9%**	**53%**	**22%**	**70%**
0-200 kg m^{-2}s^{-1}	8	30%	42%	44%	41%	40%	13%	13%	46%	34%	75%
200-400 kg m^{-2}s^{-1}	11	28%	8%	10%	23%	7%	7%	7%	58%	13%	68%
R142b	**20**	**17%**	**19%**	**18%**	**26%**	**20%**	**6%**	**8%**	**46%**	**18%**	**73%**
9-10 mm	**20**	**17%**	**19%**	**18%**	**26%**	**20%**	**6%**	**8%**	**46%**	**18%**	**73%**
0-200 kg m^{-2}s^{-1}	10	11%	33%	29%	30%	31%	9%	9%	42%	30%	75%
200-400 kg m^{-2}s^{-1}	10	23%	6%	8%	22%	8%	4%	7%	50%	5%	71%
R152a	**286**	**90%**	**50%**	**35%**	**37%**	**41%**	**40%**	**41%**	**43%**	**52%**	**58%**
0-1 mm	**95**	**110 %**	**37%**	**25%**	**26%**	**31%**	**30%**	**31%**	**45%**	**41%**	**62%**
200-400 kg m^{-2}s^{-1}	35	122%	21%	19%	19%	20%	19%	19%	54%	22%	69%
400-600 kg m^{-2}s^{-1}	31	105%	33%	20%	24%	27%	25%	27%	41%	40%	61%
600-800 kg m^{-2}s^{-1}	29	100%	63%	38%	38%	49%	47%	49%	37%	63%	55%
1-2 mm	**80**	**111 %**	**77%**	**60%**	**63%**	**66%**	**64%**	**66%**	**42%**	**74%**	**57%**
200-400 kg m^{-2}s^{-1}	24	104%	32%	34%	34%	32%	32%	32%	53%	31%	69%
400-600 kg m^{-2}s^{-1}	29	131%	86%	73%	80%	82%	79%	81%	38%	90%	55%

600-800 kg $m^{-2}s^{-1}$	19	84%	77%	50%	51%	59%	57%	58%	38%	72%	56%
800-1000 kg $m^{-2}s^{-1}$	8	126%	178%	116%	112 %	130%	127%	130%	30%	151%	33%
3-4 mm	**40**	**38%**	**17%**	**7%**	**11%**	**12%**	**12%**	**12%**	**49%**	**25%**	**63%**
0-200 kg $m^{-2}s^{-1}$	12	73%	16%	14%	16%	11%	11%	11%	58%	17%	63%
200-400 kg $m^{-2}s^{-1}$	12	39%	19%	6%	8%	14%	14%	14%	49%	26%	62%
400-600 kg $m^{-2}s^{-1}$	16	10%	17%	2%	9%	12%	11%	12%	42%	30%	64%
4-5 mm	**71**	**69%**	**54%**	**38%**	**36%**	**44%**	**41%**	**42%**	**38%**	**59%**	**50%**
0-200 kg $m^{-2}s^{-1}$	35	71%	30%	26%	24%	26%	21%	21%	44%	33%	58%
200-400 kg $m^{-2}s^{-1}$	24	77%	69%	45%	45%	57%	57%	57%	32%	80%	45%
400-600 kg $m^{-2}s^{-1}$	12	48%	87%	57%	50%	70%	69%	70%	36%	97%	40%
R161	**45**	**55%**	**12%**	**17%**	**15%**	**14%**	**14%**	**14%**	**48%**	**24%**	**65%**
2-3 mm	**45**	**55%**	**12%**	**17%**	**15%**	**14%**	**14%**	**14%**	**48%**	**24%**	**65%**
200-400 kg $m^{-2}s^{-1}$	35	63%	13%	18%	15%	15%	15%	15%	48%	24%	65%
400-600 kg $m^{-2}s^{-1}$	10	27%	7%	13%	13%	9%	10%	9%	49%	21%	65%
R32	**1060**	**115 %**	**28%**	**29%**	**28%**	**39%**	**31%**	**39%**	**47%**	**48%**	**60%**
0-1 mm	**366**	**140 %**	**18%**	**19%**	**16%**	**41%**	**24%**	**38%**	**41%**	**53%**	**57%**
0-200 kg $m^{-2}s^{-1}$	36	136%	36%	48%	34%	34%	44%	37%	34%	25%	80%
200-400 kg $m^{-2}s^{-1}$	100	183%	9%	9%	8%	21%	10%	19%	47%	34%	62%
400-600 kg $m^{-2}s^{-1}$	103	147%	19%	17%	15%	49%	26%	46%	40%	65%	54%
600-800 kg $m^{-2}s^{-1}$	70	149%	33%	31%	26%	69%	42%	65%	30%	86%	44%
800-1000 kg $m^{-2}s^{-1}$	35	54%	7%	4%	6%	31%	12%	28%	48%	45%	61%
1000-1200 kg $m^{-2}s^{-1}$	22	30%	11%	3%	9%	28%	9%	25%	49%	42%	62%
1-2 mm	**455**	**111 %**	**30%**	**33%**	**26%**	**34%**	**26%**	**29%**	**40%**	**39%**	**64%**
0-200 kg $m^{-2}s^{-1}$	196	97%	31%	42%	24%	29%	24%	20%	26%	22%	75%
200-400 kg $m^{-2}s^{-1}$	168	113%	25%	22%	26%	25%	20%	24%	58%	37%	64%
400-600 kg $m^{-2}s^{-1}$	71	120%	28%	26%	25%	50%	30%	47%	41%	66%	54%
600-800 kg $m^{-2}s^{-1}$	20	199%	65%	61%	46%	110%	78%	106%	23%	135%	22%
2-3 mm	**35**	**83%**	**9%**	**14%**	**12%**	**20%**	**13%**	**19%**	**50%**	**29%**	**63%**
200-400 kg $m^{-2}s^{-1}$	30	92%	9%	14%	12%	22%	13%	21%	49%	31%	62%
400-600 kg $m^{-2}s^{-1}$	5	31%	14%	16%	18%	7%	8%	6%	52%	18%	65%
3-4 mm	**46**	**244 %**	**65%**	**65%**	**128 %**	**88%**	**135%**	**150%**	**166%**	**95%**	**62%**
0-200 kg $m^{-2}s^{-1}$	12	861%	251%	228%	463 %	258%	477%	501%	486%	240%	71%

200-400 kg $m^{-2}s^{-1}$	8	60%	9%	5%	8%	27%	12%	25%	45%	43%	56%
400-600 kg $m^{-2}s^{-1}$	26	16%	11%	8%	10%	29%	15%	27%	56%	45%	61%
4-5 mm	**128**	**41%**	**39%**	**36%**	**32%**	**46%**	**38%**	**44%**	**51%**	**56%**	**56%**
0-200 kg $m^{-2}s^{-1}$	28	43%	24%	31%	25%	28%	22%	24%	57%	28%	66%
200-400 kg $m^{-2}s^{-1}$	55	45%	35%	32%	33%	36%	33%	35%	54%	42%	62%
400-600 kg $m^{-2}s^{-1}$	21	46%	43%	40%	39%	53%	45%	51%	49%	65%	56%
600-800 kg $m^{-2}s^{-1}$	12	29%	55%	48%	38%	83%	61%	80%	38%	108%	38%
800-1000 kg $m^{-2}s^{-1}$	12	22%	60%	52%	27%	88%	65%	85%	37%	114%	37%
9-10 mm	**20**	**28%**	**21%**	**29%**	**33%**	**26%**	**12%**	**14%**	**48%**	**29%**	**67%**
0-200 kg $m^{-2}s^{-1}$	10	33%	38%	49%	45%	36%	18%	13%	44%	27%	74%
200-400 kg $m^{-2}s^{-1}$	10	23%	10%	10%	22%	16%	7%	15%	51%	31%	62%
11-12 mm	**10**	**22%**	**33%**	**39%**	**41%**	**17%**	**5%**	**11%**	**33%**	**11%**	
0-200 kg $m^{-2}s^{-1}$	10	22%	33%	39%	41%	17%	5%	11%	33%	11%	
R404A	**13**	**20%**	**29%**	**24%**	**22%**	**36%**	**13%**	**36%**	**38%**	**41%**	**58%**
5-6 mm	**13**	**20%**	**29%**	**24%**	**22%**	**36%**	**13%**	**36%**	**38%**	**41%**	**58%**
0-200 kg $m^{-2}s^{-1}$	5	14%	41%	39%	37%	14%	6%	23%	33%	13%	70%
200-400 kg $m^{-2}s^{-1}$	4	28%	18%	9%	20%	28%	3%	24%	50%	35%	64%
400-600 kg $m^{-2}s^{-1}$	4	21%	24%	21%	5%	70%	32%	65%	34%	83%	51%
R41	**38**	**171 %**	**22%**	**36%**	**18%**	**124%**	**22%**	**107%**	**43%**	**113%**	**38%**
2-3 mm	**38**	**171 %**	**22%**	**36%**	**18%**	**124%**	**22%**	**107%**	**43%**	**113%**	**38%**
200-400 kg $m^{-2}s^{-1}$	28	184%	22%	37%	18%	127%	24%	110%	45%	114%	39%
400-600 kg $m^{-2}s^{-1}$	10	134%	23%	34%	16%	117%	16%	101%	40%	107%	35%
R410A	**217**	**133 %**	**39%**	**37%**	**38%**	**59%**	**46%**	**63%**	**47%**	**71%**	**52%**
0-1 mm	**54**	**340 %**	**44%**	**30%**	**39%**	**70%**	**44%**	**72%**	**45%**	**88%**	**51%**
0-200 kg $m^{-2}s^{-1}$	18	402%	29%	7%	27%	36%	28%	50%	55%	62%	61%
200-400 kg $m^{-2}s^{-1}$	36	309%	49%	41%	45%	87%	52%	83%	41%	100%	47%
3-4 mm	**34**	**77%**	**15%**	**18%**	**28%**	**37%**	**34%**	**49%**	**65%**	**44%**	**62%**
0-200 kg $m^{-2}s^{-1}$	6	250%	55%	57%	104 %	60%	125%	142%	118%	55%	71%
200-400 kg $m^{-2}s^{-1}$	12	62%	8%	9%	11%	22%	9%	20%	51%	30%	63%
400-600 kg $m^{-2}s^{-1}$	16	22%	8%	10%	12%	39%	19%	36%	55%	49%	61%
4-5 mm	**113**	**67%**	**44%**	**46%**	**40%**	**68%**	**55%**	**69%**	**45%**	**80%**	**50%**
0-200 kg $m^{-2}s^{-1}$	22	86%	18%	18%	18%	31%	35%	51%	37%	35%	59%
200-400 kg $m^{-2}s^{-1}$	46	70%	46%	47%	47%	62%	51%	58%	49%	70%	54%

400-600 kg $m^{-2}s^{-1}$	21	75%	56%	59%	55%	82%	66%	78%	52%	98%	48%
600-800 kg $m^{-2}s^{-1}$	12	42%	42%	54%	39%	98%	69%	94%	40%	118%	41%
800-1000 kg $m^{-2}s^{-1}$	12	27%	58%	58%	28%	103%	73%	99%	36%	126%	37%
11-12 mm	**16**	**19%**	**37%**	**36%**	**40%**	**11%**	**5%**	**19%**	**34%**	**13%**	
0-200 kg $m^{-2}s^{-1}$	16	19%	37%	36%	40%	11%	5%	19%	34%	13%	
R448A	**15**	**34%**	**17%**	**17%**	**18%**	**19%**	**25%**	**35%**	**31%**	**23%**	**62%**
5-6 mm	**15**	**34%**	**17%**	**17%**	**18%**	**19%**	**25%**	**35%**	**31%**	**23%**	**62%**
0-200 kg $m^{-2}s^{-1}$	7	45%	27%	25%	25%	5%	33%	43%	15%	3%	64%
200-400 kg $m^{-2}s^{-1}$	4	29%	11%	6%	16%	20%	11%	18%	51%	28%	62%
400-600 kg $m^{-2}s^{-1}$	4	19%	6%	12%	6%	41%	24%	39%	40%	54%	61%
R449A	**14**	**28%**	**17%**	**21%**	**12%**	**24%**	**25%**	**40%**	**30%**	**29%**	**60%**
5-6 mm	**14**	**28%**	**17%**	**21%**	**12%**	**24%**	**25%**	**40%**	**30%**	**29%**	**60%**
0-200 kg $m^{-2}s^{-1}$	7	37%	26%	28%	15%	6%	29%	41%	16%	4%	64%
200-400 kg $m^{-2}s^{-1}$	3	24%	7%	7%	17%	21%	6%	19%	54%	29%	64%
400-600 kg $m^{-2}s^{-1}$	4	17%	15%	20%	5%	57%	34%	54%	37%	73%	54%
R450A	**106**	**33%**	**12%**	**9%**	**15%**	**20%**	**15%**	**21%**	**39%**	**33%**	**61%**
4-5 mm	**106**	**33%**	**12%**	**9%**	**15%**	**20%**	**15%**	**21%**	**39%**	**33%**	**61%**
0-200 kg $m^{-2}s^{-1}$	7	51%	14%	20%	11%	10%	30%	34%	24%	8%	66%
200-400 kg $m^{-2}s^{-1}$	39	34%	12%	11%	17%	20%	13%	18%	43%	31%	61%
400-600 kg $m^{-2}s^{-1}$	60	30%	11%	7%	15%	21%	15%	21%	38%	37%	61%
R452B	**141**	**85%**	**13%**	**15%**	**18%**	**34%**	**19%**	**30%**	**43%**	**45%**	**59%**
0-1 mm	**69**	**153 %**	**13%**	**14%**	**11%**	**46%**	**26%**	**44%**	**35%**	**58%**	**55%**
200-400 kg $m^{-2}s^{-1}$	22	231%	14%	11%	11%	39%	20%	37%	34%	50%	54%
400-600 kg $m^{-2}s^{-1}$	23	145%	12%	15%	11%	49%	28%	46%	34%	61%	55%
600-800 kg $m^{-2}s^{-1}$	12	106%	12%	17%	11%	52%	30%	49%	33%	65%	54%
800-1000 kg $m^{-2}s^{-1}$	12	70%	15%	16%	12%	49%	28%	46%	41%	61%	58%
8-9 mm	**72**	**21%**	**13%**	**15%**	**25%**	**22%**	**12%**	**18%**	**51%**	**32%**	**63%**
0-200 kg $m^{-2}s^{-1}$	8	23%	39%	49%	46%	34%	15%	9%	44%	29%	73%
200-400 kg $m^{-2}s^{-1}$	29	19%	19%	19%	26%	9%	10%	7%	56%	15%	67%
400-600 kg $m^{-2}s^{-1}$	27	22%	7%	3%	19%	29%	11%	27%	49%	44%	61%
600-800 kg $m^{-2}s^{-1}$	8	20%	7%	6%	20%	36%	17%	34%	47%	55%	58%
R454C	**223**	**53%**	**22%**	**18%**	**17%**	**52%**	**31%**	**56%**	**30%**	**66%**	**48%**
4-5 mm	**209**	**54%**	**22%**	**18%**	**17%**	**53%**	**31%**	**56%**	**30%**	**67%**	**48%**
0-200 kg $m^{-2}s^{-1}$	20	95%	16%	16%	18%	21%	53%	74%	16%	28%	49%

200-400 kg $m^{-2}s^{-1}$	95	66%	23%	18%	20%	54%	29%	53%	32%	68%	48%
400-600 kg $m^{-2}s^{-1}$	94	33%	23%	18%	14%	59%	28%	56%	30%	74%	48%
5-6 mm	**14**	**44%**	**21%**	**17%**	**12%**	**38%**	**43%**	**60%**	**29%**	**51%**	**54%**
0-200 kg $m^{-2}s^{-1}$	6	64%	9%	15%	11%	14%	55%	69%	16%	23%	57%
200-400 kg $m^{-2}s^{-1}$	4	40%	16%	7%	10%	42%	21%	39%	45%	54%	56%
400-600 kg $m^{-2}s^{-1}$	4	19%	42%	30%	16%	71%	46%	68%	34%	90%	50%
R455A	**179**	**105 %**	**26%**	**22%**	**17%**	**54%**	**39%**	**56%**	**29%**	**73%**	**47%**
0-1 mm	**77**	**220 %**	**41%**	**33%**	**28%**	**74%**	**51%**	**71%**	**18%**	**94%**	**42%**
200-400 kg $m^{-2}s^{-1}$ kg $m^{-2}s^{-1}$	31	319%	41%	33%	30%	73%	50%	70%	11%	93%	36%
400-600 kg $m^{-2}s^{-1}$	22	193%	35%	30%	23%	70%	48%	67%	18%	90%	43%
600-800 kg $m^{-2}s^{-1}$	12	131%	43%	35%	29%	76%	54%	73%	28%	94%	48%
800-1000 kg $m^{-2}s^{-1}$	12	106%	52%	37%	31%	80%	57%	77%	26%	99%	47%
5-6 mm	**11**	**50%**	**23%**	**22%**	**19%**	**53%**	**57%**	**78%**	**34%**	**64%**	**47%**
0-200 kg $m^{-2}s^{-1}$	5	74%	3%	10%	11%	23%	66%	83%	18%	33%	50%
200-400 kg $m^{-2}s^{-1}$	3	42%	26%	20%	24%	62%	36%	58%	52%	72%	49%
400-600 kg $m^{-2}s^{-1}$	3	19%	48%	44%	27%	94%	63%	90%	43%	109%	44%
8-9 mm	**91**	**14%**	**14%**	**13%**	**8%**	**38%**	**26%**	**41%**	**37%**	**56%**	**53%**
0-200 kg $m^{-2}s^{-1}$	11	26%	20%	26%	25%	5%	29%	40%	12%	10%	61%
200-400 kg $m^{-2}s^{-1}$	38	14%	10%	7%	7%	35%	19%	34%	46%	51%	56%
400-600 kg $m^{-2}s^{-1}$	35	12%	14%	15%	5%	49%	30%	47%	36%	72%	51%
600-800 kg $m^{-2}s^{-1}$	7	7%	18%	21%	6%	58%	38%	56%	36%	83%	49%
R513A	**58**	**257 %**	**66%**	**71%**	**61%**	**103%**	**90%**	**101%**	**31%**	**114%**	**38%**
0-1 mm	**25**	**190 %**	**11%**	**12%**	**11%**	**27%**	**23%**	**26%**	**26%**	**35%**	**59%**
200-400 kg $m^{-2}s^{-1}$	12	195%	7%	8%	12%	18%	15%	18%	31%	26%	62%
400-600 kg $m^{-2}s^{-1}$	13	187%	15%	17%	10%	35%	31%	34%	22%	44%	57%
1-2 mm	**33**	**308 %**	**107%**	**115%**	**99%**	**161%**	**140%**	**158%**	**34%**	**173%**	**23%**
400-600 kg $m^{-2}s^{-1}$	33	308%	107%	115%	99%	161%	140%	158%	34%	173%	23%

4.3 Correlation performance for synthetic refrigerants in enhanced tubes

Figure A.2 presents the microfin tube correlation data and the MAE values are presented in Table 7. Both correlations have an overall prediction of under 50%, with Chamra et al. [77]

being better at 27%. This is likely because the Chamra et al. [77] correlation incorporates more fin geometry (e.g., fin height, number of fins, apex angle and helix angle of the microfin tube). There is no R1234ze(Z) data presented for the Chamra et al. [77] correlation because the paper does not present the apex angle for the tube. The Kedzierski and Goncalves [57] correlation created two versions—one using the Jakob number and one without. Due to the lack of reported wall temperatures, the correlation without the Jakob number was used here. The HFO data was predicted fairly well (~25% for Chamra et al. [77], ~33% for Kedzierski and Goncalves [57]). The low GWP HFC refrigerants were predicted less accurately, with R32 predicted a little better than R152a. There were not HFC/HFO mixture data presented in microfin tubes.

Table 7 Mean average error (MAE) predictions of synthetic refrigerant data for enhanced tubes, where "Original MAE" refers to the MAE reported in the original paper

	Chamra et al. [77]	Kedzierski and Goncalves [57]
Original	25%	31%
R1234yf	25%	31%
R1234ze(E)	23%	34%
R1234ze(Z)	N/A	36%
R134a	24%	33%
R152a	38%	61%
R32	31%	54%
R404A	N/A	53%
R410A	42%	57%
R448A	N/A	31%
R449A	N/A	26%
R454C	N/A	27%
R455A	N/A	28%

4.4 Correlation performance for natural refrigerants in smooth tubes

Data were separated into smooth and enhanced tube data and run through their respective correlations. A brief discussion of the correlations' predictions follows. The Akers et al. [87] correlation (Figure B.1a) was the second best for ammonia, although not recommended for CO_2

and propane due to overpredictions; MAE between experimental data and predictions are reported in Table 8 and are color coded: green (MAE ≤ 20%), yellow (20%<MAE<50%), and red (MAE > 50%). The Cavallini et al. [83] correlation over predicted ammonia and CO_2. The subsequent Cavallini et al. [85] improved the ammonia prediction, over predicted CO_2, and appeared to underpredict the data from Fonk and Garimella [96, 99] even more than the previous. The Kim and Mudawar [35] correlation developed for mini-channels had the second best overall MAE calculated and is the only correlation that had two refrigerants within the 20% error range, with the best prediction for propane. The Macdonald and Garimella [89] correlation developed for larger tubes (i.e., D=7.75–14.45 mm) and high pressure refrigerants generally underpredicts condensation heat transfer coefficients of the natural refrigerants, but was the best predictor of the CO_2 data.

The original Shah [34] correlation, which was not developed for natural refrigerants (Table 4), over predicts nearly all data. The only data that was not substantially over prediction was the Ammonia and CO_2 data from Fronk and Garimella [96, 99]. Shah [84] improved the correlation in 2009 and reduced the over prediction significantly for natural refrigerants. In 2013, Shah [68] released an update of his Shah [34] correlation, with similar results as the original correlation and further overprediction of high quality ammonia data. The latest Shah [67] used CO_2 in its development and offers the lowest MAE but still struggles to predict many data, particularly small diameter ammonia and CO_2 data. The Traviss et al. [69] correlation was the second worst correlation at predicting natural refrigerants, and over predicts CO_2 and propane. The Kim and Mudawar [35] correlation is recommended for propane and R600a; all correlations analyzed struggled to predict CO_2 and ammonia.

The table also breaks the predictions down by diameter and mass flux. There were not discernable patterns for quality and Reynolds number. Ammonia was poorly predicted by all correlations, with none predicting all the ammonia data better than 41% MAE. There were no real patterns that emerged from sorting by tube diameter and mass flux. However, the Shah16 and the Macdonald correlations begin to predict better for ammonia as the tube diameter increases. CO_2 was predicted even worse than ammonia with most correlations having a MAE over 80%. There could be a trend of the correlations being able to predict very low mass flux, 0-200 kg/m^{2}s, in mini-channel tubes, < 4 mm.

As for the hydrocarbons, isobutane was handled well by the correlations with most correlations having a MAE below 30%. With the exception of a couple of correlations, isobutane appears to be predictable in the 8 – 9 mm tube diameter range for low mass fluxes, 0 – 400 kg/m^{2}s. Propane was fairly predictable as well with most of the correlations having below a 40% MAE. Some of the correlations predicted well with small tube diameters, 0 – 3mm; and most predicting well for diameters > 5 mm.

Table 8 Mean average error (MAE) predictions of natural refrigerant data for smooth tubes, where "Original MAE" refers to the MAE reported in the original paper (*Due to the iterative nature of the correlation, not all data was able to be predicted.)

	# of samples	Akers	Cav06*	Cav11	Kim	Macdonald*	Shah79	Shah09	Shah13	Shah16
Ammonia	**311**	**43%**	**79%**	**52%**	**66%**	**48%**	**53%**	**62%**	**60%**	**41%**
0.001-0.002 m	**75**	**36%**	**26%**	**51%**	**36%**	**78%**	**45%**	**46%**	**45%**	**58%**
0-200 kg $m^{-2}s^{-1}$	75	36%	26%	51%	36%	78%	45%	46%	45%	58%
0.007-0.008 m	**123**	**27%**	**69%**	**41%**	**51%**	**48%**	**44%**	**50%**	**45%**	**39%**
0-200 kg $m^{-2}s^{-1}$	99	23%	63%	40%	50%	52%	41%	49%	41%	41%
200-400 kg $m^{-2}s^{-1}$	24	42%	85%	44%	52%	33%	57%	56%	59%	30%
0.008-0.009 m	**113**	**64%**	**123%**	**64%**	**103%**	**22%**	**69%**	**85%**	**86%**	**32%**
0-200 kg $m^{-2}s^{-1}$	101	62%	115%	60%	103%	24%	62%	81%	82%	31%
200-400 kg $m^{-2}s^{-1}$	12	79%	173%	101%	105%	4%	122%	119%	122%	42%
CO_2	**732**	**224%**	**85%**	**86%**	**80%**	**43%**	**134%**	**97%**	**127%**	**50%**
0-0.001 m	**420**	**313%**	**75%**	**77%**	**78%**	**49%**	**119%**	**90%**	**112%**	**49%**
200-400 kg $m^{-2}s^{-1}$	18	199%	17%	11%	8%	64%	17%	13%	16%	16%
400-600 kg $m^{-2}s^{-1}$	94	354%	68%	66%	67%	46%	109%	80%	102%	39%
600-800 kg $m^{-2}s^{-1}$	158	325%	80%	81%	81%	46%	125%	95%	118%	51%
800-1000 kg $m^{-2}s^{-1}$	150	289%	80%	89%	88%	51%	132%	101%	125%	59%
0.001-0.002 m	**58**	**218%**	**115%**	**114%**	**105%**	**21%**	**191%**	**137%**	**184%**	**34%**
400-600 kg $m^{-2}s^{-1}$	17	236%	105%	93%	95%	29%	162%	114%	156%	29%
600-800 kg $m^{-2}s^{-1}$	20	203%	99%	101%	90%	21%	175%	124%	169%	29%
800-1000 kg $m^{-2}s^{-1}$	21	219%	137%	142%	126%	16%	230%	168%	222%	44%
0.003-0.004 m	**27**	**55%**	**37%**	**33%**	**25%**	**56%**	**51%**	**45%**	**51%**	**39%**
200-400 kg $m^{-2}s^{-1}$	10	70%	23%	18%	18%	57%	30%	26%	29%	46%
400-600 kg $m^{-2}s^{-1}$	5	66%	40%	34%	27%	52%	60%	50%	59%	35%
800-1000 kg $m^{-2}s^{-1}$	12	37%	51%	45%	29%	57%	66%	59%	65%	36%
0.004-0.005 m	**35**	**105%**	**77%**	**102%**	**53%**	**68%**	**259%**	**61%**	**225%**	**94%**
400-600 kg $m^{-2}s^{-1}$	7	62%	34%	37%	24%	59%	85%	27%	73%	59%

600-800 kg $m^{-2}s^{-1}$	21	144%	111%	149%	71%	76%	374%	86%	324%	120%
800-1000 kg $m^{-2}s^{-1}$	7	32%	27%	29%	29%	50%	90%	20%	78%	53%
0.005-0.006 m	**92**	**97%**	**152%**	**158%**	**115%**	**12%**	**235%**	**187%**	**228%**	**50%**
600-800 kg $m^{-2}s^{-1}$	27	83%	126%	133%	103%	11%	208%	159%	202%	32%
800-1000 kg $m^{-2}s^{-1}$	32	95%	160%	161%	128%	14%	234%	189%	228%	56%
1000-1200 kg $m^{-2}s^{-1}$	33	109%	167%	174%	112%	11%	257%	208%	250%	60%
0.006-0.007 m	**100**	**55%**	**49%**	**51%**	**66%**	**74%**	**50%**	**44%**	**49%**	**50%**
0-200 kg $m^{-2}s^{-1}$	58	40%	52%	54%	77%	74%	42%	37%	37%	42%
200-400 kg $m^{-2}s^{-1}$	36	70%	37%	39%	42%	65%	54%	47%	59%	55%
800-1000 kg $m^{-2}s^{-1}$	6	100%	100%	100%	100%	100%	100%	100%	100%	100%
Isobutane	**61**	**17%**	**26%**	**30%**	**21%**	**69%**	**27%**	**16%**	**15%**	**38%**
0.005-0.006 m	**10**	**9%**	**48%**	**53%**	**24%**	**79%**	**48%**	**30%**	**30%**	**54%**
0-200 kg $m^{-2}s^{-1}$	10	9%	48%	53%	24%	79%	48%	30%	30%	54%
0.006-0.007 m	**10**	**17%**	**41%**	**46%**	**23%**	**76%**	**39%**	**18%**	**19%**	**45%**
0-200 kg $m^{-2}s^{-1}$	10	17%	41%	46%	23%	76%	39%	18%	19%	45%
0.007-0.008 m	**10**	**25%**	**25%**	**33%**	**28%**	**72%**	**25%**	**14%**	**14%**	**29%**
0-200 kg $m^{-2}s^{-1}$	10	25%	25%	33%	28%	72%	25%	14%	14%	29%
0.008-0.009 m	**21**	**17%**	**14%**	**7%**	**9%**	**63%**	**12%**	**12%**	**11%**	**40%**
0-200 kg $m^{-2}s^{-1}$	9	13%	9%	8%	10%	64%	9%	7%	7%	47%
200-400 kg $m^{-2}s^{-1}$	12	21%	19%	6%	8%	62%	14%	15%	14%	34%
0.01-0.011 m	**10**	**17%**	**30%**	**36%**	**35%**	**71%**	**29%**	**9%**	**9%**	**24%**
0-200 kg $m^{-2}s^{-1}$	10	17%	30%	36%	35%	71%	29%	9%	9%	24%
Propane	**303**	**94%**	**16%**	**16%**	**14%**	**59%**	**34%**	**24%**	**31%**	**35%**
0-0.001 m	**130**	**141%**	**18%**	**13%**	**10%**	**57%**	**40%**	**28%**	**38%**	**32%**
0-200 kg $m^{-2}s^{-1}$	19	312%	7%	4%	8%	61%	23%	14%	22%	24%
200-400 kg $m^{-2}s^{-1}$	26	223%	22%	17%	16%	56%	39%	29%	38%	30%
400-600 kg $m^{-2}s^{-1}$	30	120%	17%	13%	9%	53%	46%	32%	44%	30%

600-800 kg $m^{-2}s^{-1}$	22	74%	16%	11%	9%	57%	40%	28%	38%	34%
800-1000 kg $m^{-2}s^{-1}$	22	49%	25%	15%	8%	59%	45%	33%	43%	38%
1000-1200 kg $m^{-2}s^{-1}$	11	27%	28%	15%	7%	61%	45%	33%	43%	45%
0.001-0.002 m	**49**	**101%**	**17%**	**16%**	**17%**	**59%**	**35%**	**25%**	**33%**	**38%**
200-400 kg $m^{-2}s^{-1}$	27	104%	16%	15%	19%	64%	22%	16%	20%	45%
400-600 kg $m^{-2}s^{-1}$	22	97%	18%	18%	15%	54%	51%	36%	49%	30%
0.002-0.003 m	**57**	**65%**	**9%**	**10%**	**9%**	**62%**	**27%**	**20%**	**26%**	**43%**
200-400 kg $m^{-2}s^{-1}$	47	72%	10%	11%	8%	62%	28%	21%	27%	43%
400-600 kg $m^{-2}s^{-1}$	10	35%	5%	6%	11%	62%	23%	16%	22%	40%
0.005-0.006 m	**10**	**10%**	**48%**	**54%**	**27%**	**76%**	**43%**	**15%**	**12%**	**38%**
0-200 kg $m^{-2}s^{-1}$	10	10%	48%	54%	27%	76%	43%	15%	12%	38%
0.006-0.007 m	**10**	**23%**	**35%**	**43%**	**23%**	**71%**	**29%**	**8%**	**10%**	**28%**
0-200 kg $m^{-2}s^{-1}$	10	23%	35%	43%	23%	71%	29%	8%	10%	28%
0.007-0.008 m	**10**	**33%**	**22%**	**30%**	**24%**	**66%**	**13%**	**14%**	**18%**	**24%**
0-200 kg $m^{-2}s^{-1}$	10	33%	22%	30%	24%	66%	13%	14%	18%	24%
0.008-0.009 m	**27**	**21%**	**9%**	**7%**	**14%**	**61%**	**26%**	**28%**	**26%**	**44%**
0-200 kg $m^{-2}s^{-1}$	9	14%	11%	12%	15%	62%	19%	12%	20%	45%
200-400 kg $m^{-2}s^{-1}$	18	24%	8%	5%	13%	61%	30%	36%	29%	43%
0.01-0.011 m	**10**	**28%**	**29%**	**34%**	**42%**	**65%**	**17%**	**24%**	**30%**	**14%**
0-200 kg $m^{-2}s^{-1}$	10	28%	29%	34%	42%	65%	17%	24%	30%	14%

4.5 Correlation performance for natural refrigerants in enhanced tubes

Three data sets (Kim et al. [103], Son and Oh [104], and Vollrath et al. [98]) included enhanced tubes. The data from Vollrath et al. [98] were excluded from further consideration due to the fact that the authors noted their large fins and wide fin spacing likely increased the refrigerant thermal resistance layer instead of decreasing it. The remaining data were compared to the

enhanced tube correlations of Chamra et al. [77] and Kedzierski and Goncalves [57], of which the Kedzierski and Goncalves [57] was 20 times more accurate (Table 9).

Table 9 Mean average error (MAE) predictions of natural refrigerant data for enhanced tubes

	Chamra et al. [77]	Kedzierski and Goncalves [57]
Original	20%	23.50%
Ammonia (R717)	N/A	N/A
CO_2 (R744)	596%	30%
Propane (R290)	N/A	N/A
R600a	N/A	N/A

5. Conclusions and future opportunities

Smooth tube correlations analyzed in this paper include Akers et al. [87], Cavallini et al. [83], Cavallini et al. [85], Kim and Mudawar [35], Macdonald and Garimella [89], Shah [34], Shah [84], Shah [68], Shah [67], and Traviss et al. [69] and enhanced tube correlations developed by Chamra et al. [77] and Kedzierski and Goncalves [57]. For these corrleations, MAE values were tabulated and color coded for synthetic refrigerants in smooth tubes (Table 6), synthetic refrigerants in enhanced tubes (Table 7), natural refrigerants in smooth tubes (Table 8), and natural refrigerants in enhanced tubes (Table 9). The smooth tube tables also break MAEs down by diameter and mass flux. Quality and liquid-only Reynolds number were also analyzed, but no discernable patterns were found. There is a strong correlation of performance capability and diameter. The correlations developed with macro-scale tubes did not predict mini-scale tubes well. For synthetic refrigerants, Cavallini et al. [85] and Kim and Mudawar [35] were the best predictors for emerging synthetic refrigerants (e.g., R1234yf, R1234ze(E), R32, R450A, R513A, etc.). The Kim and Mudawar [35] correlation is recommended for propane and R600a; although the Macdonald and Garimella [89] had the lowest MAE for CO_2 at 43%, most correlations analyzed could not predict the heat transfer

coefficient for CO_2 and ammonia. For microfin tubes, data were more limited, but the Chamra et al. [77] correlation incorporated more microfin geometry and was a better predictor for synthetic refrigerants while the Kedzierski and Goncalves [57] correlation was a better predictor for natural refrigerants.

Some correlations have large MAEs since the current refrigerant condensation data are beyond the ranges considered in the studies; for example, the Akers *et al*. [87] correlation has been developed with only two refrigerants (i.e., R290 and R12) in a 15.8-mm diameter tube and its MAE is high for most refrigerants, likely due to the small tube diameters and alternate fluids in the condensation database. This shows to be true since Akers et al. [87] has much larger MAEs for diameters less than 4 mm. However, there are a few examples where the refrigerant data were within the correlation's specified design parameters (i.e., diameter, mass flux, temperature), but were poorly predicted. The Kim and Mudawar [35] correlation was developed for diameter ranges between 0.424 mm and 6.22 mm, and the R513A data falls within that range with 0.71 mm to 1.16 mm diameter data, yet the MAE was 61% for R513A. The Kim and Mudawar [35] correlation has been developed with R134a and R513A data, so the thermodynamic properties are not unique to the correlation. Two observations are that the R513A data are limited [15, 52] and all R513A condensation data are in multiport extruded aluminum tubing, which could impact flow regimes and heat transfer dynamics. A second example is the prediction of R513A data using the Cavallini *et al.* [83] correlation. The R513A data falls within the diameter ranges of this correlation (i.e., 0.69 mm to 7.79 mm). The Cavallini *et al.* [83] correlation has been developed with refrigerants, including R134a, but the study did not include R1234yf. The physics of flow within multiport extruded aluminum tubes possibly had an impact on the heat transfer coefficients; this also indicates that for emerging refrigerants, additional condensation data are needed in various

geometries. An example on the natural refrigerant side is the CO_2 data of Heo *et al.* [100] for prediction with the Kim and Mudawar [35] correlation. The data of Heo *et al.* [100] (i.e., 0.68 mm to 1.5 mm) fits within the Kim and Mudawar [35] correlation diameter range, yet the MAE was 98%. The Kim and Mudawar [35] correlation has been developed with CO_2, so the high pressures of CO_2 are unlikely the reason for the large predictive error. The Heo *et al.* [100] data were for condensation in multiport extruded aluminum tubing, so that is a possible explanation for the discrepancy. Both the Kim and Mudawar [35] and the Cavallini *et al.* [83] correlations were developed with multiport tube data, highlighting the difficulty in predicting the physics involved in multiport tube flow.

Opportunities for future work include:

- Report wall temperatures in research papers or post tabulated data: Most of the existing studies have not included wall temperature which can be considered a potential deficiency, as such comprehensive reporting is critical to fully understand the experimental procedure and to facilitate the application.
- Limited condensation flow data for emerging synthetic fluids and blends: Some emerging refrigerants have very limited flow condensation data available in open literature so additional experiments are warranted.
- Limited condensation flow data for natural fluids: There is limited research investigating the flow condensation with natural refrigerants in small diameter tubes, and further studies would be a beneficial contribution to the literature.
- Most of the existing correlations are empirical formulations where no specific attention has been paid to the fundamental physics. While such correlation include specific fluid properties, since they are developed for specific flow conditions and working fluid, it is

really unrealizable to use the same correlations for additional tube geometries and refrigerants.

- Development of universal correlation for condensation heat transfer: a comprehensive condensation performance correlation is required to unify the existing studies in a manner that overall information can be used in rather simplistic manner without need for large amounts of computing power.

Acknowledgements

The authors gratefully acknowledge the financial support of National Science Foundation grants 1603737 (INTERN supplement) and 1828571.

References

[1] Birmpili, T., 2018, "Montreal Protocol at 30: The governance structure, the evolution, and the Kigali Amendment," Comptes Rendus Geoscience, 350(7), pp. 425-431.
[2] Egger Haysmith, S., and Nijman, S., 2019, "Kigali Amendment implementation begins."
[3] Purohit, P., Höglund Isaksson, L., and Wagner, F., 2018, "Impacts of the Kigali Amendment to phase-down hydrofluorocarbons (HFCs) in Asia," International Institute for Applied Systems Analysis.
[4] Höglund-Isaksson, L., Purohit, P., Amann, M., Bertok, I., Rafaj, P., Schöpp, W., and Borken-Kleefeld, J., 2017, "Cost estimates of the Kigali Amendment to phase-down hydrofluorocarbons," Environmental Science & Policy, 75, pp. 138-147.
[5] Nawaz, K., and Ally, M. R., 2019, "Options for low-global-warming-potential and natural refrigerants Part 2: Performance of refrigerants and systemic irreversibilities," International Journal of Refrigeration, 106, pp. 213-224.
[6] Ally, M. R., Sharma, V., and Nawaz, K., 2019, "Options for low-global-warming-potential and natural refrigerants part I: Constrains of the shape of the P–T and T–S saturation phase boundaries," International Journal of Refrigeration, 106, pp. 144-152.
[7] Nawaz, K., Shen, B., Elatar, A., Baxter, V., and Abdelaziz, O., 2018, "Performance optimization of CO2 heat pump water heater," International Journal of Refrigeration, 85, pp. 213-228.
[8] Nawaz, K., Shen, B., Elatar, A., Baxter, V., and Abdelaziz, O., 2017, "R1234yf and R1234ze (E) as low-GWP refrigerants for residential heat pump water heaters," International Journal of Refrigeration, 82, pp. 348-365.
[9] Nawaz, K., Shen, B., Elatar, A., Baxter, V., and Abdelaziz, O., 2017, "R290 (propane) and R600a (isobutane) as natural refrigerants for residential heat pump water heaters," Applied Thermal Engineering, 127, pp. 870-883.
[10] ASHRAE, 2017, Fundamentals Handbook.

[11] Azzolin, M., Berto, A., Bortolin, S., Moro, L., and Del Col, D., 2019, "Condensation of ternary low GWP zeotropic mixtures inside channels," International Journal of Refrigeration, 103, pp. 77-90.
[12] Del Col, D., Torresin, D., and Cavallini, A., 2010, "Heat transfer and pressure drop during condensation of the low GWP refrigerant R1234yf," International Journal of Refrigeration, 33(7), pp. 1307-1318.
[13] Del Col, D., Bortolato, M., Azzolin, M., and Bortolin, S., 2015, "Condensation heat transfer and two-phase frictional pressure drop in a single minichannel with R1234ze (E) and other refrigerants," International Journal of Refrigeration, 50, pp. 87-103.
[14] Longo, G. A., Mancin, S., Righetti, G., and Zilio, C., 2019, "Saturated vapour condensation of R134a inside a 4 mm ID horizontal smooth tube: Comparison with the low GWP substitutes R152a, R1234yf and R1234ze (E)," International Journal of Heat and Mass Transfer, 133, pp. 461-473.
[15] López-Belchí, A., 2019, "Assessment of a mini-channel condenser at high ambient temperatures based on experimental measurements working with R134a, R513A and R1234yf," Applied Thermal Engineering, 155, pp. 341-353.
[16] Wang, L., Dang, C., and Hihara, E., 2012, "Experimental study on condensation heat transfer and pressure drop of low GWP refrigerant HFO1234yf in a horizontal tube," International Journal of Refrigeration, 35(5), pp. 1418-1429.
[17] Yang, C.-Y., and Nalbandian, H., 2018, "Condensation heat transfer and pressure drop of refrigerants HFO-1234yf and HFC-134a in small circular tube," International Journal of Heat and Mass Transfer, 127, pp. 218-227.
[18] Diani, A., Campanale, M., Cavallini, A., and Rossetto, L., 2018, "Low GWP refrigerants condensation inside a 2.4 mm ID microfin tube," International Journal of Refrigeration, 86, pp. 312-321.
[19] Diani, A., Cavallini, A., and Rossetto, L., 2017, "R1234yf condensation inside a 3.4 mm ID horizontal microfin tube," International Journal of Refrigeration, 75, pp. 178-189.
[20] Del Col, D., Azzolin, M., Bortolin, S., and Zilio, C., 2015, "Two-phase pressure drop and condensation heat transfer of R32/R1234ze (E) non-azeotropic mixtures inside a single microchannel," Science and Technology for the Built Environment, 21(5), pp. 595-606.
[21] Hossain, M. A., Onaka, Y., and Miyara, A., 2012, "Experimental study on condensation heat transfer and pressure drop in horizontal smooth tube for R1234ze (E), R32 and R410A," International Journal of Refrigeration, 35(4), pp. 927-938.
[22] Li, M., Guo, Q., Lv, J., and Li, D., 2018, "Research on condensation heat transfer characteristics of R447A, R1234ze, R134a and R32 in multi-port micro-channel tubes," International Journal of Heat and Mass Transfer, 118, pp. 637-650.
[23] Miyara, A., Afroz, H. M., and Hossain, M. A., "In-tube condensation of low GWP mixture refrigerants R1234ze (E)/R32," Proc. International Heat Transfer Conference, Begel House Inc., pp. 737-750.
[24] Guo, Q., Li, M., and Gu, H., 2018, "Condensation heat transfer characteristics of low-GWP refrigerants in a smooth horizontal mini tube," International Journal of Heat and Mass Transfer, 126, pp. 26-38.
[25] Jige, D., Inoue, N., and Koyama, S., 2016, "Condensation of refrigerants in a multiport tube with rectangular minichannels," International Journal of Refrigeration, 67, pp. 202-213.

[26] Liu, N., Xiao, H., and Li, J., 2016, "Experimental investigation of condensation heat transfer and pressure drop of propane, R1234ze (E) and R22 in minichannels," Applied Thermal Engineering, 102, pp. 63-72.
[27] Rossato, M., Da Silva, J., Ribatski, G., and Del Col, D., 2017, "Heat transfer and pressure drop during condensation of low-GWP refrigerants inside bar-and-plate heat exchangers," International Journal of Heat and Mass Transfer, 114, pp. 363-379.
[28] Toninelli, P., Bortolin, S., Azzolin, M., and Del Col, D., 2019, "Effects of geometry and fluid properties during condensation in minichannels: experiments and simulations," Heat and Mass Transfer, 55(1), pp. 41-57.
[29] Kondou, C., Mishima, F., and Koyama, S., 2015, "Condensation and evaporation of R32/R1234ze (E) and R744/R32/R1234ze (E) flow in horizontal microfin tubes," Science and Technology for the Built Environment, 21(5), pp. 564-577.
[30] Kondou, C., Mishima, F., Liu, J., and Koyama, S., 2014, "Condensation and evaporation of R744/R32/R1234ze (E) flow in horizontal microfin tubes," International Refrigeration and Air Conditioning Conference, Purdue University, West Lafayette, IN, pp. 1-10.
[31] Kondou, C., Mishima, F., Liu, J., and Koyama, S., 2014, "Condensation and evaporation of R134a, R1234ze (E) and R1234ze (Z) flow in horizontal microfin tubes at higher temperature," International Refrigeration and Air Conditioning Conference, Purdue University, West Lafayette, IN, pp. 1-10.
[32] "Honeywell: Solstice® ze Refrigerant (HFO-1234ze), The Environmental Alternative to Traditional Refrigerants," https://www.honeywell-refrigerants.com/india/?document=solstice-ze-hfo-1234ze-brochure-2012&download=1.
[33] Righetti, G., Zilio, C., Mancin, S., and Longo, G. A., 2016, "A review on in-tube two-phase heat transfer of hydro-fluoro-olefines refrigerants," Science and Technology for the Built Environment, 22(8), pp. 1191-1225.
[34] Shah, M. M., 1979, "A general correlation for heat transfer during film condensation inside pipes," International Journal of Heat and Mass Transfer, 22(4), pp. 547-556.
[35] Kim, S.-M., and Mudawar, I., 2013, "Universal approach to predicting heat transfer coefficient for condensing mini/micro-channel flow," International Journal of Heat and Mass Transfer, 56(1-2), pp. 238-250.
[36] Haraguchi, H., Koyama, S., and Fujii, T., 1994, "Condensation of Refrigerants HCFC 22, HFC 134a and HCFC 123 in a Horizontal Smooth Tube:(2nd Report, Proposals of Empirical Expressions for Local Heat Transfer Coefficient)," Transactions of the Japan Society of Mechanical Engineers Series B, 60(574), pp. 2117-2124.
[37] Dobson, M., and Chato, J., 1998, "Condensation in smooth horizontal tubes," Journal of Heat Transfer, 120, pp. 193-213.
[38] Wang, W.-W. W., Radcliff, T. D., and Christensen, R. N., 2002, "A condensation heat transfer correlation for millimeter-scale tubing with flow regime transition," Experimental Thermal and Fluid Science, 26(5), pp. 473-485.
[39] Koyama, S., Kuwahara, K., and Nakashita, K., "Condensation of refrigerant in a multi-port channel," Proc. International Conference on Nanochannels, Microchannels, and Minichannels, pp. 193-205.
[40] Cavallini, A., Col, D. D., Doretti, L., Matkovic, M., Rossetto, L., Zilio, C., and Censi, G., 2006, "Condensation in horizontal smooth tubes: A new heat transfer model for heat exchanger design," Heat Transfer Engineering, 27(8), pp. 31-38.

[41] Park, J. E., Vakili-Farahani, F., Consolini, L., and Thome, J. R., 2011, "Experimental study on condensation heat transfer in vertical minichannels for new refrigerant R1234ze (E) versus R134a and R236fa," Experimental Thermal and Fluid Science, 35(3), pp. 442-454.
[42] Del Col, D., Bortolato, M., Azzolin, M., and Bortolin, S., 2014, "Effect of inclination during condensation inside a square cross section minichannel," International Journal of Heat and Mass Transfer, 78, pp. 760-777.
[43] Guo, S.-p., Wu, Z., Li, W., Kukulka, D., Sundén, B., Zhou, X.-p., Wei, J.-j., and Simon, T., 2015, "Condensation and evaporation heat transfer characteristics in horizontal smooth, herringbone and enhanced surface EHT tubes," International Journal of Heat and Mass Transfer, 85, pp. 281-291.
[44] Hirose, M., Ichinose, J., and Inoue, N., 2018, "Development of the general correlation for condensation heat transfer and pressure drop inside horizontal 4 mm small-diameter smooth and microfin tubes," International Journal of Refrigeration, 90, pp. 238-248.
[45] Jung, D., Song, K.-h., Cho, Y., and Kim, S.-j., 2003, "Flow condensation heat transfer coefficients of pure refrigerants," International Journal of Refrigeration, 26(1), pp. 4-11.
[46] Kukulka, D. J., Smith, R., and Li, W., 2015, "Comparison of tubeside condensation and evaporation characteristics of smooth and enhanced heat transfer 1EHT tubes," Applied Thermal Engineering, 89, pp. 1079-1086.
[47] Liu, N., and Li, J., 2015, "Experimental study on condensation heat transfer of R32, R152a and R22 in horizontal minichannels," Applied Thermal Engineering, 90, pp. 763-773.
[48] Longo, G. A., Mancin, S., Righetti, G., and Zilio, C., 2018, "Saturated vapour condensation of R410A inside a 4 mm ID horizontal smooth tube: Comparison with the low GWP substitute R32," International Journal of Heat and Mass Transfer, 125, pp. 702-709.
[49] Matkovic, M., Cavallini, A., Del Col, D., and Rossetto, L., 2009, "Experimental study on condensation heat transfer inside a single circular minichannel," International Journal of Heat and Mass Transfer, 52(9-10), pp. 2311-2323.
[50] Liu, N., Li, J. M., Sun, J., and Wang, H. S., 2013, "Heat transfer and pressure drop during condensation of R152a in circular and square microchannels," Experimental Thermal and Fluid Science, 47, pp. 60-67.
[51] Jacob, T. A., Matty, E. P., and Fronk, B. M., 2019, "Experimental investigation of in-tube condensation of low GWP refrigerant R450A using a fiber optic distributed temperature sensor," International Journal of Refrigeration, 103, pp. 274-286.
[52] Morrow, J. A., Booth, J., and Derby, M. M., 2018, "Comparison of mini-channel condensation heat transfer for R513A and R134a," International Refrigeration and Air Conditioning Conference, Purdue University, West Lafayette, IN, pp. 1-10.
[53] Agarwal, R., and Hrnjak, P., 2015, "Condensation in two phase and desuperheating zone for R1234ze (E), R134a and R32 in horizontal smooth tubes," International Journal of Refrigeration, 50, pp. 172-183.
[54] Thome, J. R., El Hajal, J., and Cavallini, A., 2003, "Condensation in horizontal tubes, Part 2: New heat transfer model based on flow regimes," International Journal of Heat and Mass Transfer, 46(18), pp. 3365-3387.
[55] Del Col, D., Cavallini, A., and Thome, J. R., 2005, "Condensation of zeotropic mixtures in horizontal tubes: New simplified heat transfer model based on flow regimes," Journal of Heat Transfer, 127(3), pp. 221-230.

[56] Cavallini, A., Del Col, D., Mancin, S., and Rossetto, L., 2009, "Condensation of pure and near-azeotropic refrigerants in microfin tubes: A new computational procedure," International Journal of Refrigeration, 32(1), pp. 162-174.
[57] Kedzierski, M., and Goncalves, J., 1999, "Horizontal convective condensation of alternative refrigerants within a micro-fin tube," Journal of Enhanced Heat Transfer, 6(2-4).
[58] Diani, A., and Rossetto, L., "HFO 1234ze (E) Condensation inside a mini microfin tube with 4.0 mm OD," Proc. International Heat Transfer Conference, Begel House Inc., pp. 2355-2360.
[59] Baird, J., Fletcher, D., and Haynes, B., 2003, "Local condensation heat transfer rates in fine passages," International Journal of Heat and Mass Transfer, 46(23), pp. 4453-4466.
[60] Garimella, S., Agarwal, A., and Bandhauer, T. M., "Channel Size Based Measurement Techniques for Condensation Heat Transfer Coefficients in Mini-and Micro-Channels," Proc. ASME International Mechanical Engineering Congress and Exposition, pp. 521-528.
[61] Moser, K., Webb, R., and Na, B., 1998, "A new equivalent Reynolds number model for condensation in smooth tubes," Transactions of the American Society of Mechanical Engineering, 120, pp. 410-417.
[62] Bandhauer, T. M., Agarwal, A., and Garimella, S., 2006, "Measurement and modeling of condensation heat transfer coefficients in circular microchannels," Transactions of the American Society of Mechanical Engineers, 128, pp. 1050-1059.
[63] Cavallini, A., Del Col, D., Doretti, L., Matkovic, M., Rossetto, L., and Zilio, C., "A model for condensation inside minichannels," Proc. Heat Transfer Summer Conference, American Society of Mechanical Engineers, pp. 297-304.
[64] Cavallini, A., Censi, G., Del Col, D., Doretti, L., Longo, G. A., and Rossetto, L., 2002, "Intube condensation of halogenated refrigerants," ASHRAE Transactions, 108(1), pp. 146-161.
[65] Cavallini, A., Censi, G., Del Col, D., Doretti, L., Longo, G., Rossetto, L., and Zilio, C., 2003, "Condensation inside and outside smooth and enhanced tubes—a review of recent research," International Journal of Refrigeration, 26(4), pp. 373-392.
[66] Jacob, T. A., and Fronk, B. M., 2020, "In-Tube condensation of zeotropic refrigerant R454C from superheated vapor to subcooled liquid," Science and Technology for the Built Environment, 26(9), pp. 1177-1190.
[67] Shah, M. M., 2016, "A correlation for heat transfer during condensation in horizontal mini/micro channels," International Journal of Refrigeration, 64, pp. 187-202.
[68] Shah, M. M., 2013, "General correlation for heat transfer duringcondensation in plain tubes: further development andverification," ASHRAE Transactions, 119(2), pp. 3-11.
[69] Traviss, D., Rohsenow, W., and Baron, A., 1973, "Forced-convection condensation inside tubes: A heat transfer equation for condenser design," ASHRAE Transactions, 79(1), pp. 157-165.
[70] Akers, W., "Condensation inside horizontal tubes," Proc. Chemical Engineering Progress Symposium Series, p. 145.
[71] Soliman, M., Schuster, J., and Berenson, P., 1968, "A general heat transfer correlation for annular flow condensation," Journal of Heat Transfer, 90(2), pp. 267-274.
[72] Tandon, T., Varma, H., and Gupta, C., 1985, "An experimental investigation of forced convection condensation during annular flow inside a horizontal tube," ASHRAE Transactions, pp. 343–354.

[73] Kim, C.-H., and Kim, N.-H., 2021, "Condensation heat transfer and pressure drop of low GWP R-404A-alternative refrigerants (R-448A, R-449A, R-455A, R-454C) in a 7.0-mm outer-diameter horizontal microfin tube," International Journal of Refrigeration, 126, pp. 181-194.
[74] Yu, J., and Koyama, S., 1998, "Condensation heat transfer of pure refrigerants in microfin tubes."
[75] Shikazono, N., Itoh, M., Uchida, M., Fukushima, T., and Hatada, T., 1998, "An analytical model to predict the condensation heat transfer coefficient in horizontal microfin tubes," ASHRAE Transactions, 104, p. 143.
[76] Tang, L., Ohadi, M. M., and Johnson, A. T., 2000, "Flow condensation in smooth and micro-fin tubes with HCFC-22, HFC-134a and HFC-410A refrigerants. Part I: experimental results," Journal of Enhanced Heat Transfer, 7(5).
[77] Chamra, L. M., Mago, P. J., Tan, M.-O., and Kung, C.-C., 2005, "Modeling of condensation heat transfer of pure refrigerants in micro-fin tubes," International Journal of Heat and Mass Transfer, 48(7), pp. 1293-1302.
[78] Han, D., and Lee, K.-J., 2005, "Experimental study on condensation heat transfer enhancement and pressure drop penalty factors in four microfin tubes," International Journal of Heat and Mass Transfer, 48(18), pp. 3804-3816.
[79] Mehendale, S. S., 2019, "Condensing heat transfer of pure refrigerants and refrigerant mixtures flowing within horizontal microfin tubes: A new model," International Journal of Refrigeration, 103, pp. 223-242.
[80] Yonemoto, R., and Koyama, S., 2007, "Experimental study on condensation of pure refrigerants in horizontal micro-fin tubes: Proposal of correlations for heat transfer coefficient and frictional pressure drop," International Refrigeration and Air Conditioning Conference, Purdue University, West Lafayette, IN, pp. 139-148.
[81] Silver, L., 1942, "Gas cooling with aqueous condensation," Transactions of the Institution of Chemical Engineers, 20(14), pp. 30–42.
[82] Bell, K. J., and Ghaly, M. A., 1973, "An approximate generalized designmethod for multicomponent/partial condenser," AIChE Symposium Series, 69, pp. 72–79.
[83] Cavallini, A., Doretti, L., Matkovic, M., and Rossetto, L., 2006, "Update on condensation heat transfer and pressure drop inside minichannels," Heat Transfer Engineering, 27(4), pp. 74-87.
[84] Shah, M. M., 2009, "An improved and extended general correlation for heat transfer during condensation in plain tubes," HVAC&R Research, 15(5), pp. 889-913.
[85] Cavallini, A., Bortolin, S., Del Col, D., Matkovic, M., and Rossetto, L., 2011, "Condensation heat transfer and pressure losses of high-and low-pressure refrigerants flowing in a single circular minichannel," Heat Transfer Engineering, 32(2), pp. 90-98.
[86] Wang, H., and Rose, J. W., 2011, "Theory of heat transfer during condensation in microchannels," International Journal of Heat and Mass Transfer, 54(11-12), pp. 2525-2534.
[87] Akers, W., Deans, H., and Crosser, O., 1959, "Condensing heat transfer within horizontal tubes," Chemical Engineering Progress Symposium Series, 55(29), pp. 171-176.
[88] Cavallini, A., and Zecchin, R., "A dimensionless correlation for heat transfer in forced convection condensation," Proc. International Heat Transfer Conference Digital Library, Begel House Inc.
[89] Macdonald, M., and Garimella, S., 2016, "Hydrocarbon condensation in horizontal smooth tubes: Part II–Heat transfer coefficient and pressure drop modeling," International Journal of Heat and Mass Transfer, 93, pp. 1248-1261.

[90] Kim, N.-H., Cho, J.-P., and Kim, J.-O., 2000, "R-22 condensation in flat aluminum multi-channel tubes," Journal of Enhanced Heat Transfer, 7(6), pp. 241-250.
[91] Zhang, M., and Webb, R. L., 2001, "Correlation of two-phase friction for refrigerants in small-diameter tubes," Experimental Thermal and Fluid Science, 25(3-4), pp. 131-139.
[92] Gebauer, T., Al-Badri, A. R., Gotterbarm, A., El Hajal, J., Leipertz, A., and Fröba, A. P., 2013, "Condensation heat transfer on single horizontal smooth and finned tubes and tube bundles for R134a and propane," International Journal of Heat and Mass Transfer, 56(1-2), pp. 516-524.
[93] Ji, W.-T., Chong, G.-H., Zhao, C.-Y., Zhang, H., and Tao, W.-Q., 2018, "Condensation heat transfer of R134a, R1234ze (E) and R290 on horizontal plain and enhanced titanium tubes," International Journal of Refrigeration, 93, pp. 259-268.
[94] Park, K.-J., and Jung, D., 2005, "Condensation heat transfer coefficients of flammable refrigerants on various enhanced tubes," Journal of Mechanical Science and Technology, 19(10), pp. 1957-1963.
[95] Jung, D., Chae, S., Bae, D., and Oho, S., 2004, "Condensation heat transfer coefficients of flammable refrigerants," International Journal of Refrigeration, 27(3), pp. 314-317.
[96] Fronk, B. M., and Garimella, S., "Heat transfer and pressure drop during condensation of ammonia in microchannels," Proc. International Conference on Micro/Nanoscale Heat Transfer, American Society of Mechanical Engineers, pp. 399-409.
[97] Komandiwirya, H. B., Hrnjak, P., and Newell, T., 2005, "An experimental investigation of pressure drop and heat transfer in an in-tube condensation system of ammonia with and without miscible oil in smooth and enhanced tubes," Air Conditioning and Refrigeration Center. College of Engineering ….
[98] Vollrath, J. E., Hrnjak, P., and Newell, T., 2003, "An experimental investigation of pressure drop and heat transfer in an in-tube condensation system of pure ammonia," Air Conditioning and Refrigeration Center. College of Engineering ….
[99] Fronk, B. M., and Garimella, S., 2016, "Condensation of carbon dioxide in microchannels," International Journal of Heat and Mass Transfer, 100, pp. 150-164.
[100] Heo, J., Park, H., and Yun, R., 2013, "Comparison of condensation heat transfer and pressure drop of CO2 in rectangular microchannels," International Journal of Heat and Mass Transfer, 65, pp. 719-726.
[101] Iqbal, O., and Bansal, P., 2012, "In-tube condensation heat transfer of CO2 at low temperatures in a horizontal smooth tube," International Journal of Refrigeration, 35(2), pp. 270-277.
[102] Kang, P., Heo, J., and Yun, R., 2013, "Condensation heat transfer characteristics of CO2 in a horizontal smooth tube," International Journal of Refrigeration, 36(3), pp. 1090-1097.
[103] Kim, Y. J., Jang, J., Hrnjak, P. S., and Kim, M. S., 2009, "Condensation heat transfer of carbon dioxide inside horizontal smooth and microfin tubes at low temperatures," Journal of Heat Transfer, 131(2).
[104] Son, C.-H., and Oh, H.-K., 2012, "Condensation heat transfer characteristics of carbon dioxide in a horizontal smooth tube," Experimental Thermal and Fluid Science, 36, pp. 233-241.
[105] Park, C. Y., and Hrnjak, P., 2009, "CO2 flow condensation heat transfer and pressure drop in multi-port microchannels at low temperatures," International Journal of Refrigeration, 32(6), pp. 1129-1139.
[106] 2014, "2013 GHGRP Industrial Profiles ".

[107] Del Col, D., Bortolato, M., and Bortolin, S., 2014, "Comprehensive experimental investigation of two-phase heat transfer and pressure drop with propane in a minichannel," International Journal of Refrigeration, 47, pp. 66-84.
[108] Del Col, D., Stefano, B., Matteo, B., and Luisa, R., 2012, "Condensation heat transfer and pressure drop with propane in a minichannel," International Refrigeration and Air Conditioning Conference, Purdue University, West Lafayette, IN, pp. 1-10.
[109] Fernando, P., Palm, B., Ameel, T., Lundqvist, P., and Granryd, E., 2008, "A minichannel aluminium tube heat exchanger–Part III: Condenser performance with propane," International Journal of Refrigeration, 31(4), pp. 696-708.
[110] Lee, H.-S., and Son, C.-H., 2010, "Condensation heat transfer and pressure drop characteristics of R-290, R-600a, R-134a and R-22 in horizontal tubes," Heat and Mass Transfer, 46(5), pp. 571-584.
[111] Park, K.-J., Jung, D., and Seo, T., 2008, "Flow condensation heat transfer characteristics of hydrocarbon refrigerants and dimethyl ether inside a horizontal plain tube," International Journal of Multiphase Flow, 34(7), pp. 628-635.
[112] Ağra, Ö., and Teke, İ., 2008, "Experimental investigation of condensation of hydrocarbon refrigerants (R600a) in a horizontal smooth tube," International Communications in Heat and Mass Transfer, 35(9), pp. 1165-1171.
[113] Ghorbani, B., Akhavan-Behabadi, M., Ebrahimi, S., and Vijayaraghavan, K., 2017, "Experimental investigation of condensation heat transfer of R600a/POE/CuO nano-refrigerant in flattened tubes," International Communications in Heat and Mass Transfer, 88, pp. 236-244.
[114] Miyara, A., 2008, "Condensation of hydrocarbons - A review," International Journal of Refrigeration, 31, pp. 621-632.
[115] Dobson, M. K., 1994, "Heat transfer and flow regimes during condensation in horizontal tubes," Air Conditioning and Refrigeration Center. College of Engineering ….
[116] Chen, M. M., 1961, "An Analytical Study of Laminar Film Condensation: Part 2—Single and Multiple Horizontal Tubes," Journal of Heat Transfer, 83(1), pp. 55-60.
[117] Tang, L., 1997, "Empirical Study of New Refrigerant Flow Condensation Inside Horizontal Smooth Tube and Micro-Fin Tubes," Ph.D. Dissertation, University of Maryland, University of Maryland College Park.
[118] Agarwal, A., Bandhauer, T. M., and Garimella, S., 2010, "Measurement and modeling of condensation heat transfer in non-circular microchannels," International Journal of Refrigeration, 33(6), pp. 1169-1179.
[119] Li, S., Han, J.-t., Su, G.-p., and Pan, J.-h., 2007, "Condensation heat transfer of R-134A in horizontal straight and helically coiled tube-in-tube heat exchangers," Journal of Hydrodynamics, Ser. B, 19(6), pp. 677-682.
[120] Bivens, D., and Yokozeki, A., 1994, "Heat transfer coefficients and transport properties for alternative refrigerants," International Refrigeration and Air Conditioning Conference, Purdue University, West Lafayette, IN, pp. 299-304.
[121] Jaster, H., and Kosky, P., 1976, "Condensation heat transfer in a mixed flow regime," International Journal of Heat and Mass Transfer, 19(1), pp. 95-99.
[122] Chen, S., Gerner, F., and Tien, C., 1987, "General film condensation correlations," Experimental Heat Transfer An International Journal, 1(2), pp. 93-107.
[123] Kondou, C., and Hrnjak, P., 2011, "Heat rejection from R744 flow under uniform temperature cooling in a horizontal smooth tube around the critical point," International Journal of Refrigeration, 34(3), pp. 719-731.

[124] Nusselt, W., 1916, "The condensation of steam on cooled surfaces," Z. Ver. Dtsch. Ing, 60, pp. 541-546.
[125] Di-an, L., and Yongren, L., 1988, "Steam condensation in vertical corrugated duct," Chemical Engineering Communications, 84(1), pp. 21-31.
[126] Kutateladze, S., 1963, Fundamentals of Heat Transfer, Academic Press, New York.
[127] Chato, J. C., 1962, "Laminar condensation inside horizontal and inclined tubes," J. ASHRAE, 4(52).
[128] Shao, W., 1993, "Condensation heat transfer in horizontal tubes: Experimental results and correlations," Proceedings of the 14th Nordic Refrigeration Conference.
[129] Dobson, M., 1994, "Experimental evaluation of internal condensation of refrigerants R-12 and R-134a," ASHRAE Transactions, pp. 744-754.
[130] Kedzierski, M. A., and Kim, M. S., 1998, "Convective Boiling and Condensation Heat Transfer With a Twisted-Tape Insert for R12, R22, R152a, R134a, R290, R32/R134a, R32/R152a, R290/R134a, R134a/R600a," Thermal Science & Engineering, 6(1), pp. 113-122.
[131] Carey, V. P., 2020, Liquid-vapor phase-change phenomena: An introduction to the thermophysics of vaporization and condensation processes in heat transfer equipment, CRC Press.
[132] Derby, M., Lee, H. J., Peles, Y., and Jensen, M. K., 2012, "Condensation heat transfer in square, triangular, and semi-circular mini-channels," International Journal of Heat and Mass Transfer, 55(1-3), pp. 187-197.

Appendix A: Experimental vs. predicted correlation graphs for synthetic refrigerants

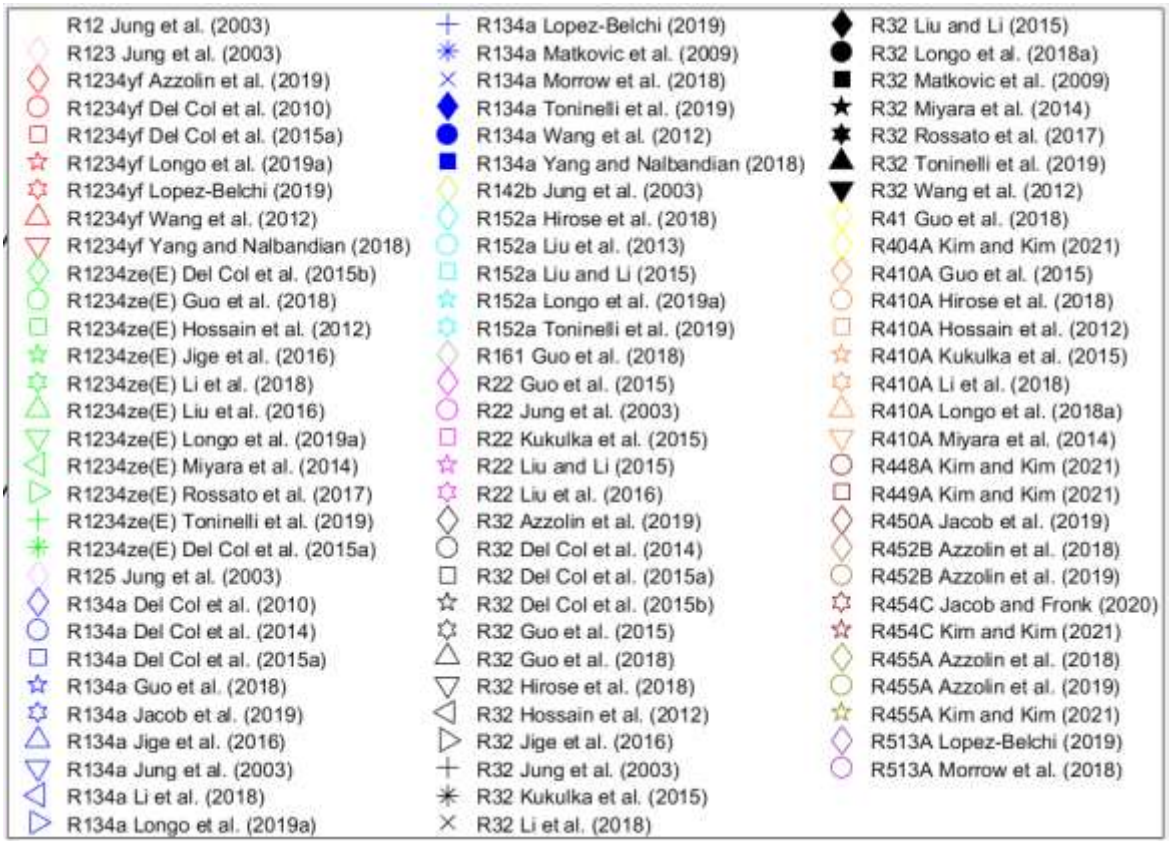

a

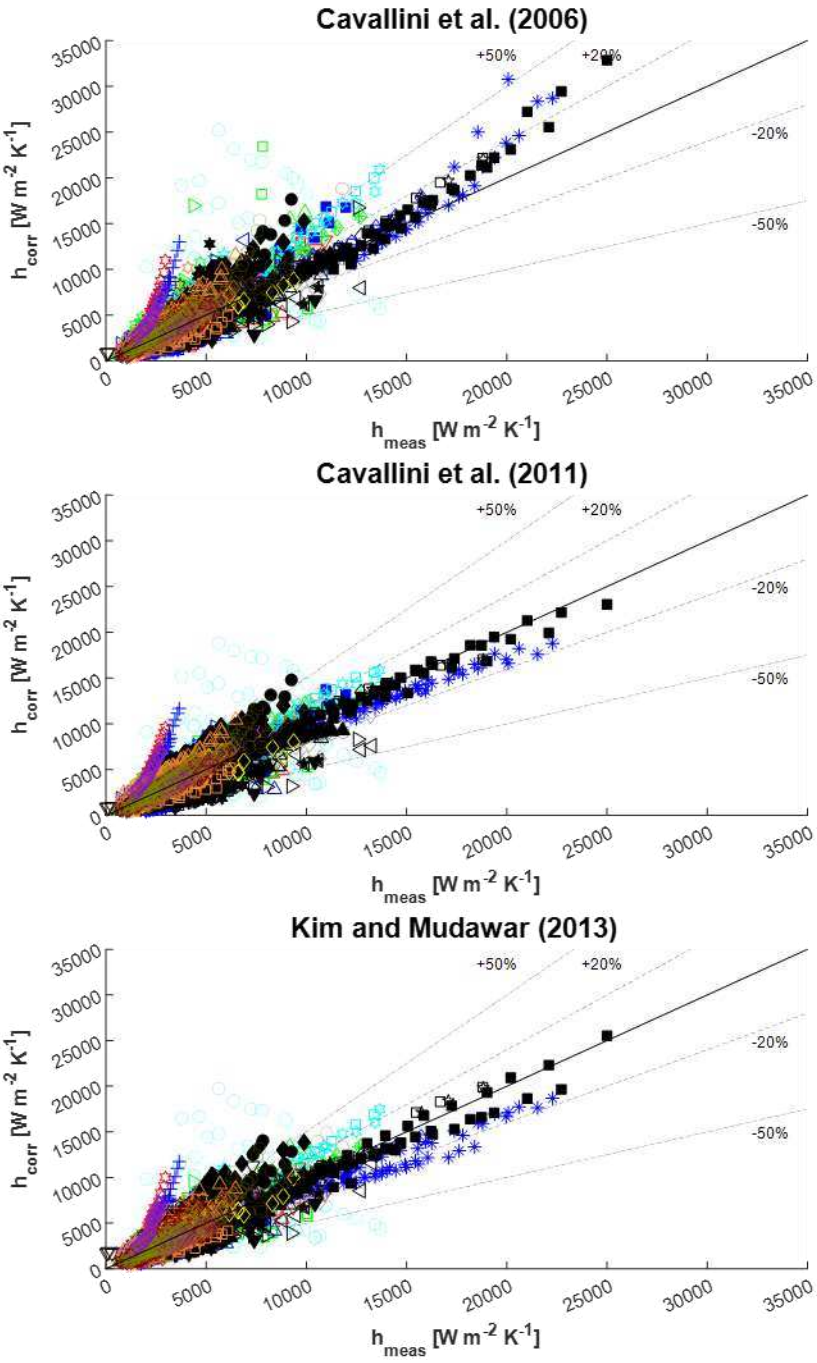
Cavallini et al. (2006)
Cavallini et al. (2011)
Kim and Mudawar (2013)
+50%
+20%
-20%
-50%
h_corr [W m^-2 K^-1]
h_meas [W m^-2 K^-1]
0
5000
10000
15000
20000
25000
30000
35000

b

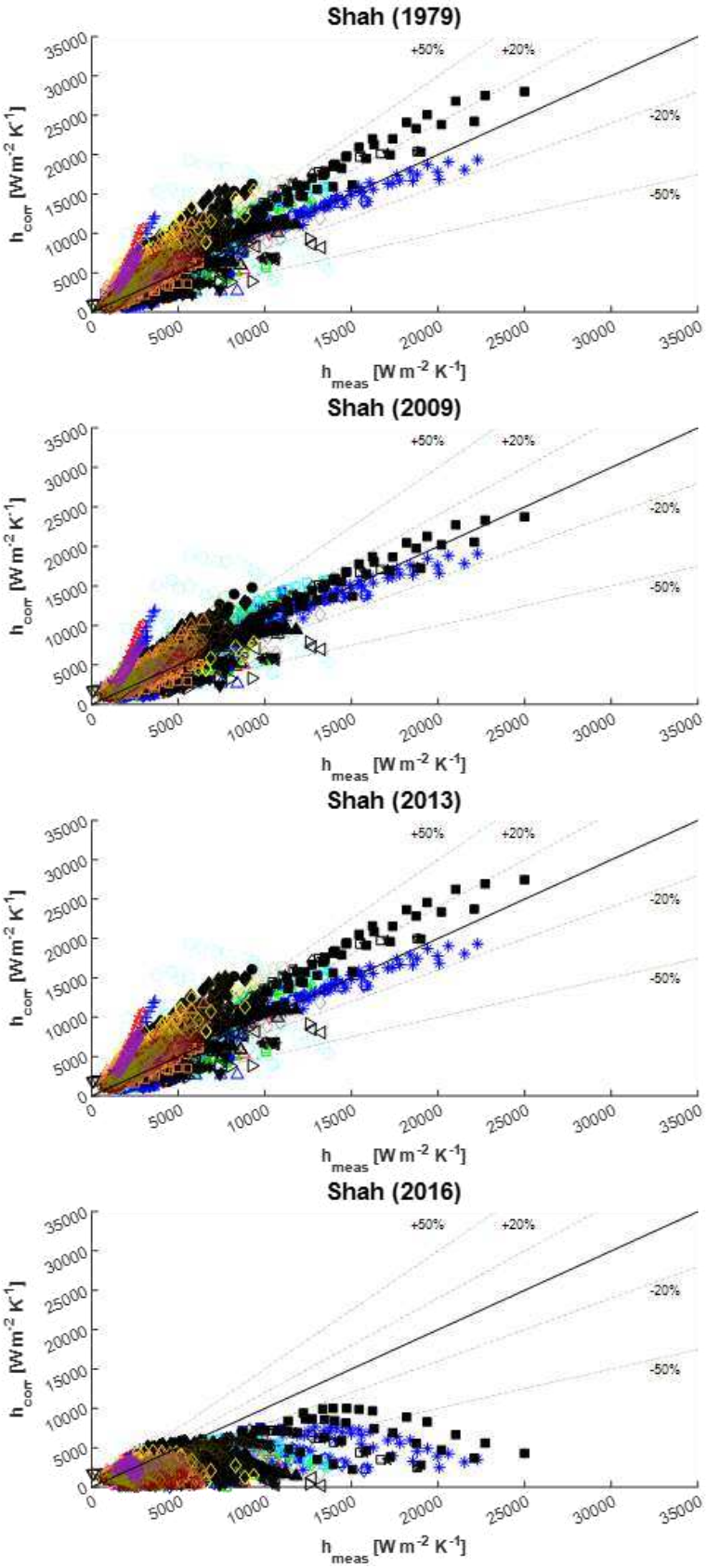
Shah (1979)
Shah (2009)
Shah (2013)
Shah (2016)
+50%
+20%
-20%
-50%
h_{corr} [W m^{-2} K^{-1}]
h_{meas} [W m^{-2} K^{-1}]
0
5000
10000
15000
20000
25000
30000
35000

c

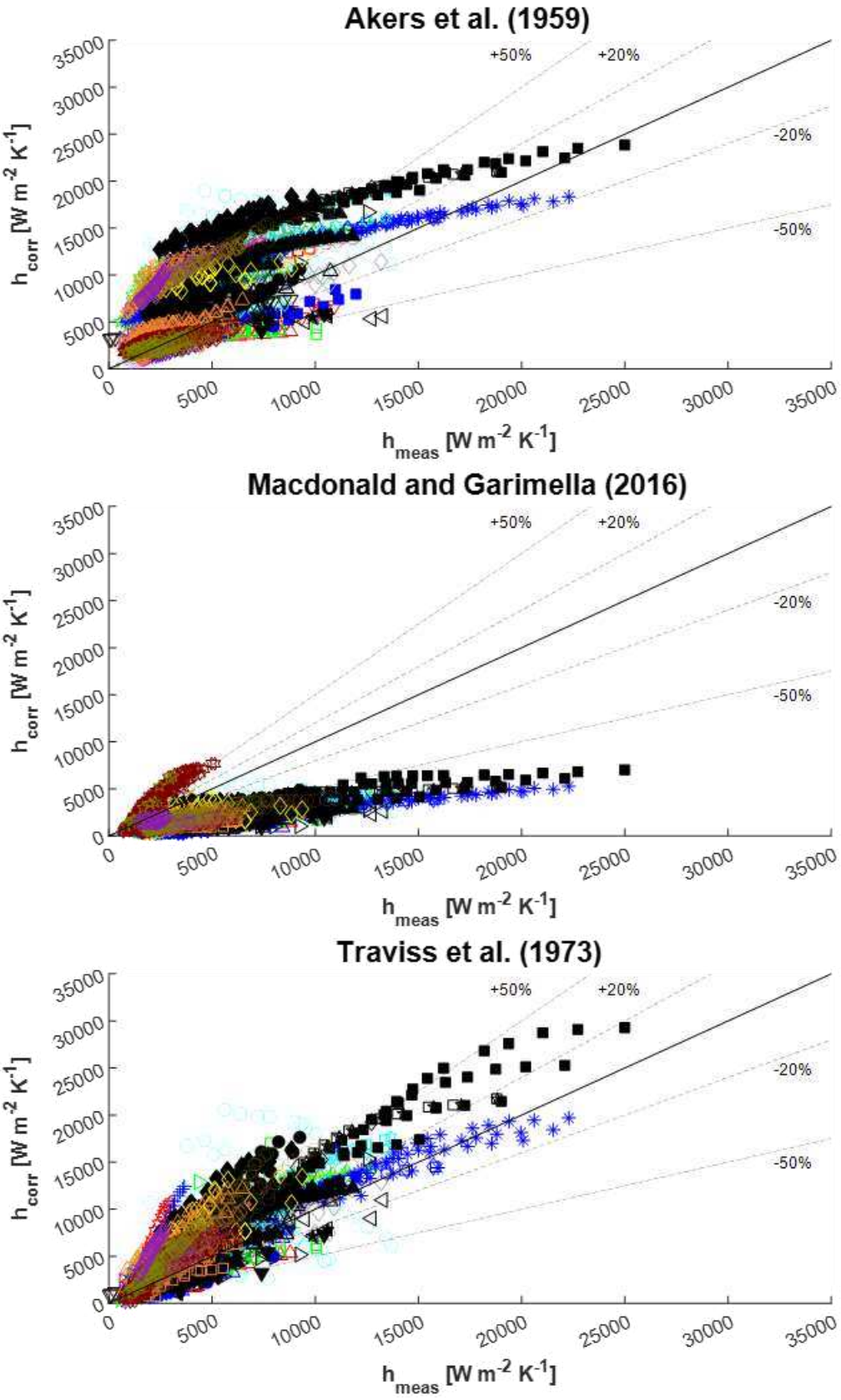
Akers et al. (1959)
Macdonald and Garimella (2016)
Traviss et al. (1973)
+50%
+20%
-20%
-50%
h_corr [W m^-2 K^-1]
h_meas [W m^-2 K^-1]
0
5000
10000
15000
20000
25000
30000
35000

Figure A.1 Predicted and experimentally-reported flow condensation from smooth tubes with synthetic refrigerants, with predictions calculated from a) Cavallini et al. [83], Cavallini et al. [85], and Kim and Mudawar [35]; b) Shah [34], Shah [84], Shah [68], and Shah [67]; and c) Akers et al. [87], Macdonald and Garimella [89], and Traviss et al. [69] correlations; all graphs share the same legend.

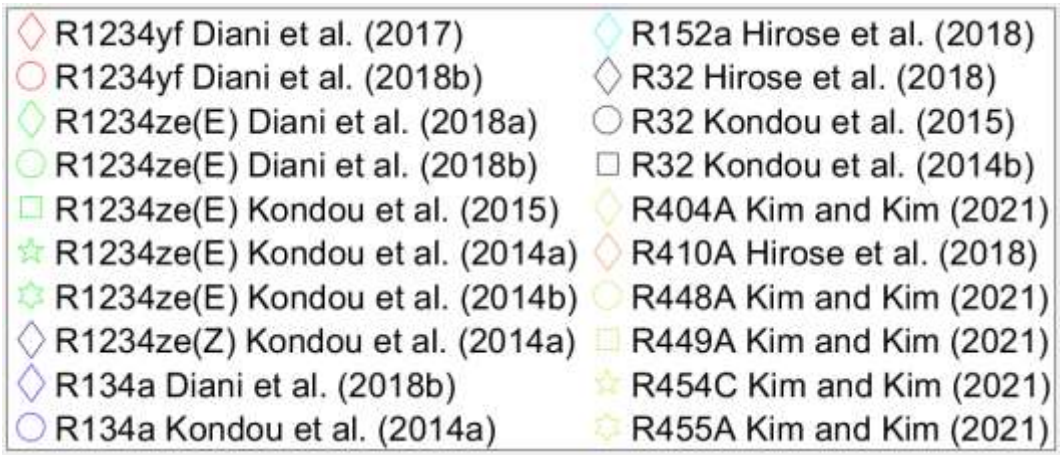

a

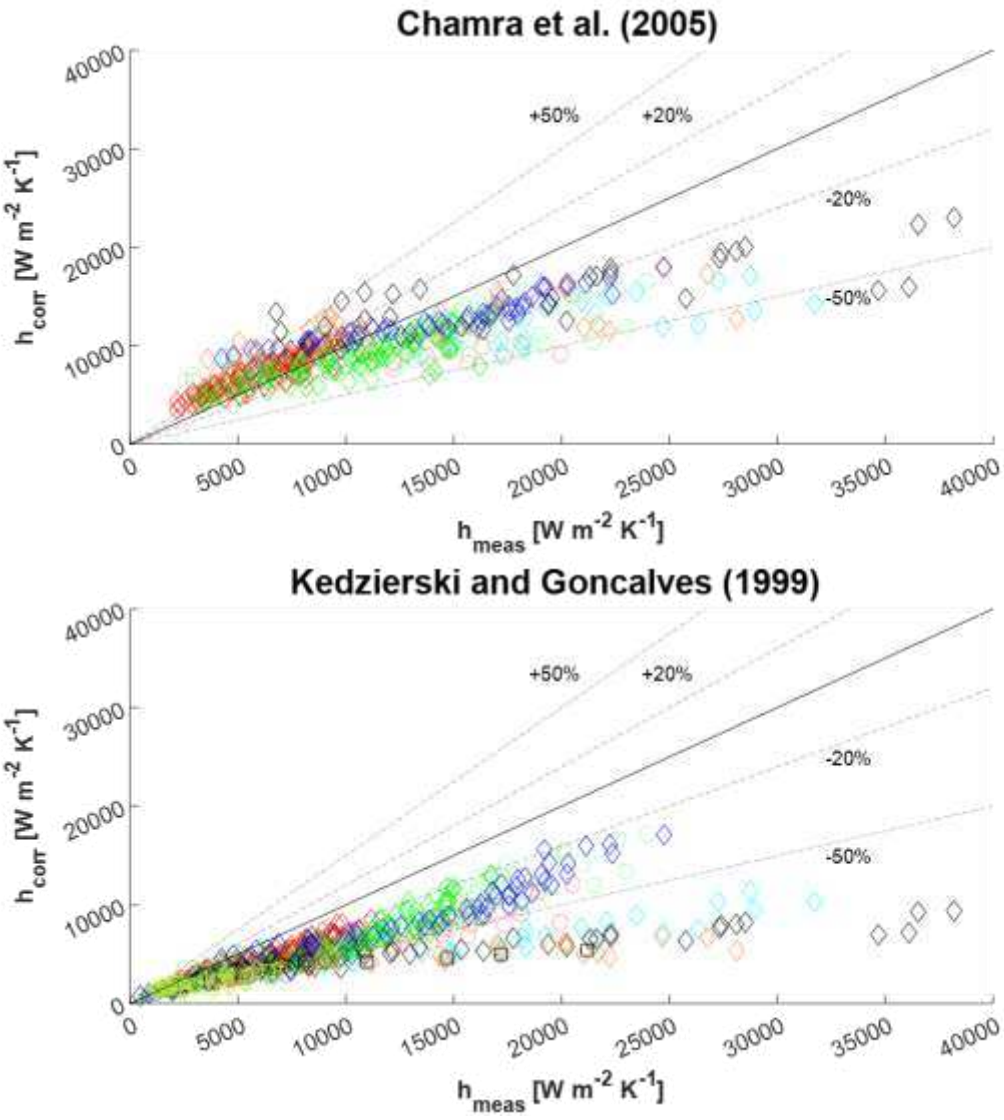

Figure A.2 Predicted and experimentally-reported flow condensation using synthetic refrigerants in enhanced tubes, with predictions calculated from Chamra et al. *[77]* and Kedzierski and Goncalves [57]

Appendix B: Experimental vs. predicted correlation graphs for natural refrigerants

a

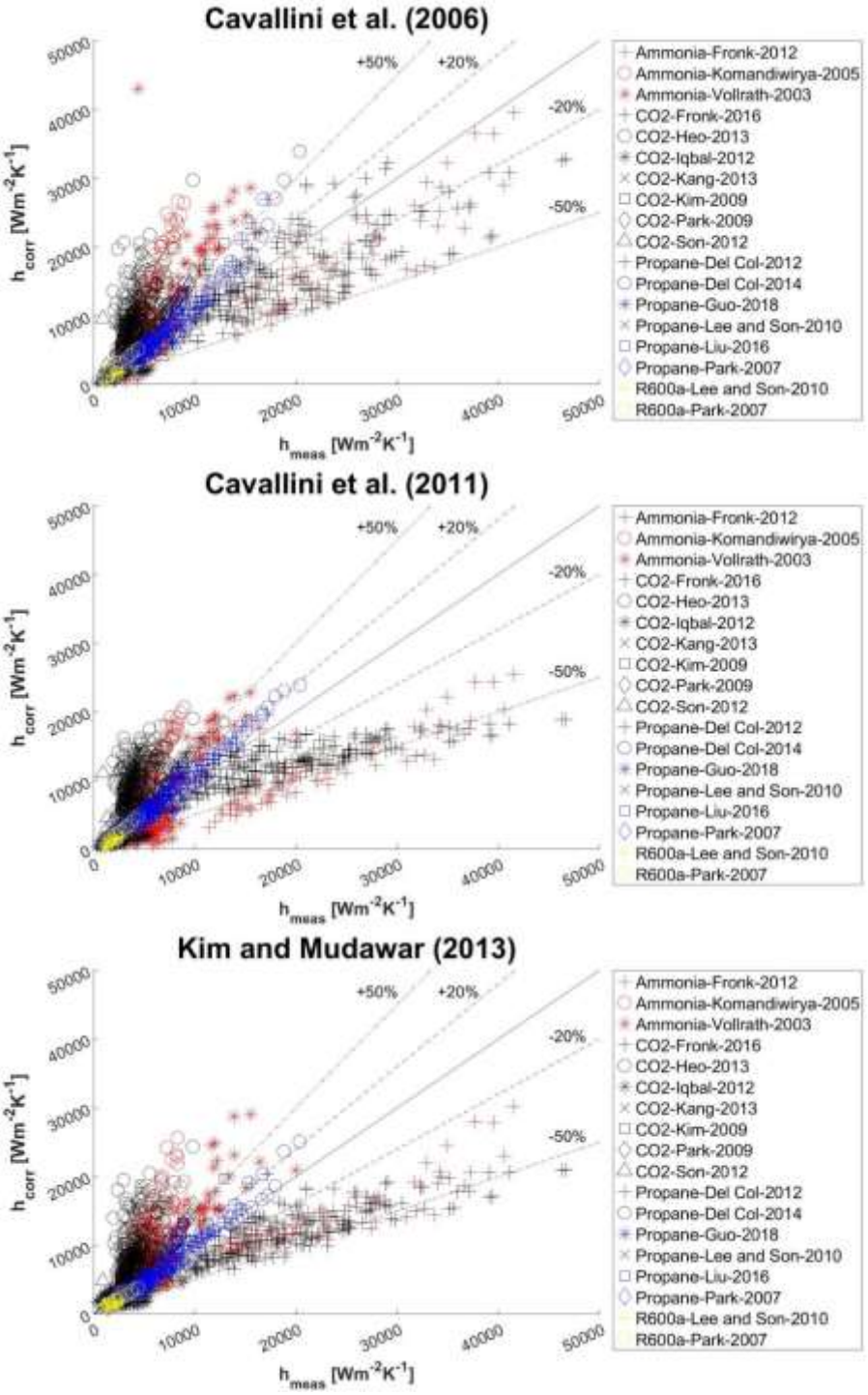
Cavallini et al. (2006)
Cavallini et al. (2011)
Kim and Mudawar (2013)
+50%
+20%
-20%
-50%
h_corr [Wm^-2K^-1]
h_meas [Wm^-2K^-1]
0
10000
20000
30000
40000
50000
Ammonia-Fronk-2012
Ammonia-Komandiwirya-2005
Ammonia-Vollrath-2003
CO2-Fronk-2016
CO2-Heo-2013
CO2-Iqbal-2012
CO2-Kang-2013
CO2-Kim-2009
CO2-Park-2009
CO2-Son-2012
Propane-Del Col-2012
Propane-Del Col-2014
Propane-Guo-2018
Propane-Lee and Son-2010
Propane-Liu-2016
Propane-Park-2007
R600a-Lee and Son-2010
R600a-Park-2007

b

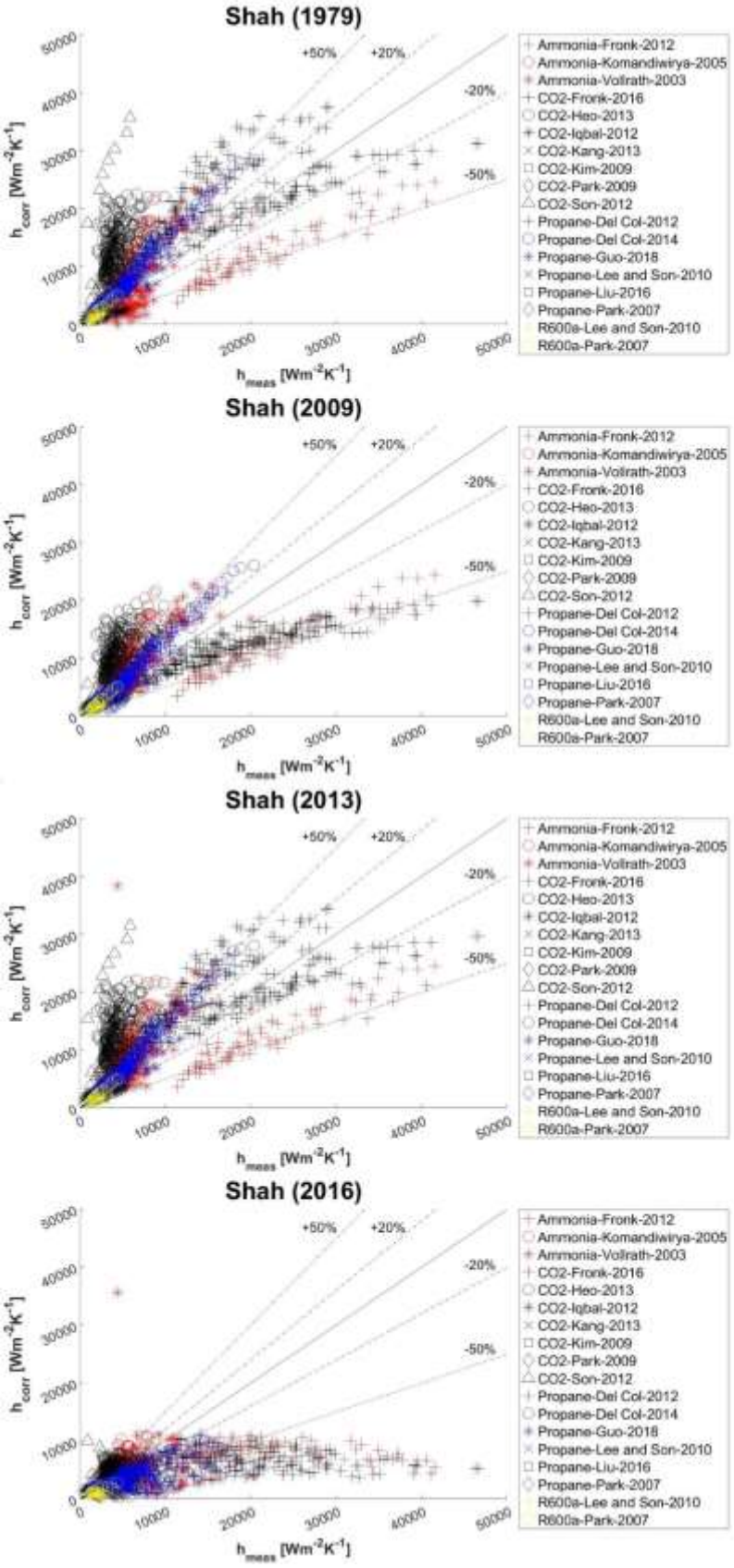
Shah (1979)
Shah (2009)
Shah (2013)
Shah (2016)
+50%
+20%
-20%
-50%
h_{corr} [Wm^{-2}K^{-1}]
h_{meas} [Wm^{-2}K^{-1}]
0
10000
20000
30000
40000
50000
Ammonia-Fronk-2012
Ammonia-Komandiwirya-2005
Ammonia-Vollrath-2003
CO2-Fronk-2016
CO2-Heo-2013
CO2-Iqbal-2012
CO2-Kang-2013
CO2-Kim-2009
CO2-Park-2009
CO2-Son-2012
Propane-Del Col-2012
Propane-Del Col-2014
Propane-Guo-2018
Propane-Lee and Son-2010
Propane-Liu-2016
Propane-Park-2007
R600a-Lee and Son-2010
R600a-Park-2007

c

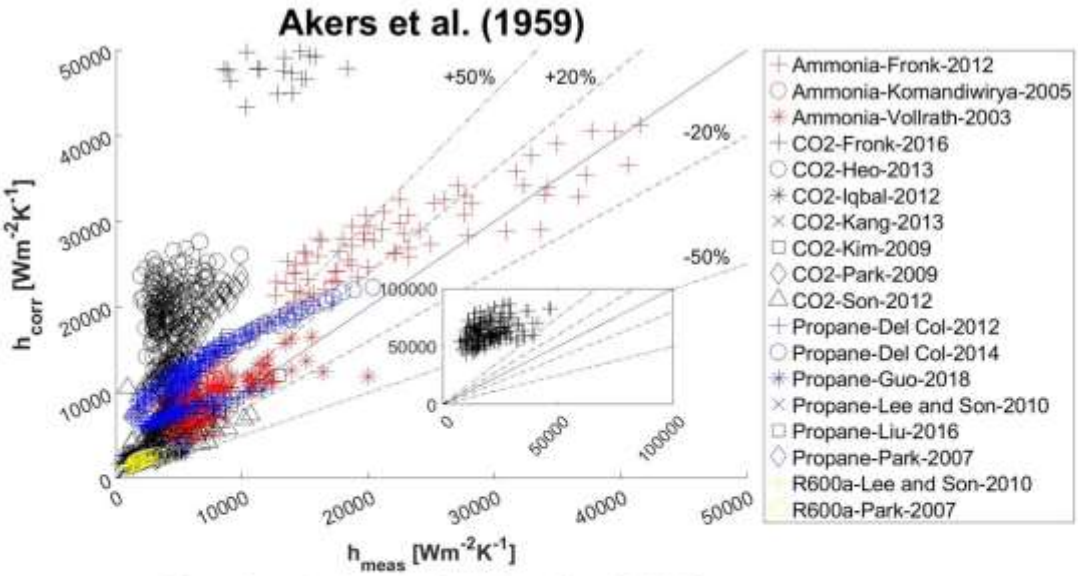
Akers et al. (1959)
+50%
+20%
-20%
-50%
h_corr [Wm^-2K^-1]
h_meas [Wm^-2K^-1]
Ammonia-Fronk-2012
Ammonia-Komandiwirya-2005
Ammonia-Vollrath-2003
CO2-Fronk-2016
CO2-Heo-2013
CO2-Iqbal-2012
CO2-Kang-2013
CO2-Kim-2009
CO2-Park-2009
CO2-Son-2012
Propane-Del Col-2012
Propane-Del Col-2014
Propane-Guo-2018
Propane-Lee and Son-2010
Propane-Liu-2016
Propane-Park-2007
R600a-Lee and Son-2010
R600a-Park-2007

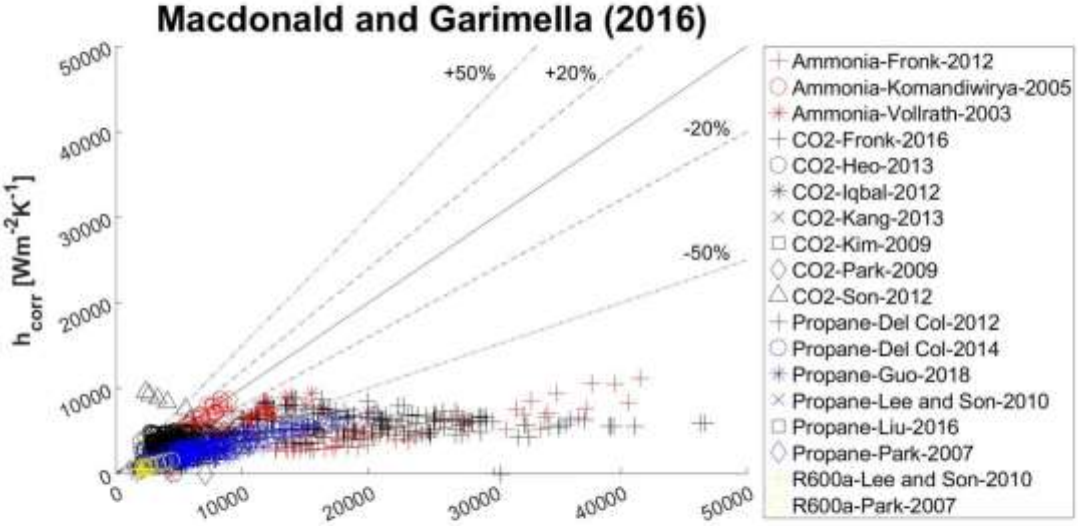
Macdonald and Garimella (2016)
+50%
+20%
-20%
-50%
h_corr [Wm^-2K^-1]
Ammonia-Fronk-2012
Ammonia-Komandiwirya-2005
Ammonia-Vollrath-2003
CO2-Fronk-2016
CO2-Heo-2013
CO2-Iqbal-2012
CO2-Kang-2013
CO2-Kim-2009
CO2-Park-2009
CO2-Son-2012
Propane-Del Col-2012
Propane-Del Col-2014
Propane-Guo-2018
Propane-Lee and Son-2010
Propane-Liu-2016
Propane-Park-2007
R600a-Lee and Son-2010
R600a-Park-2007

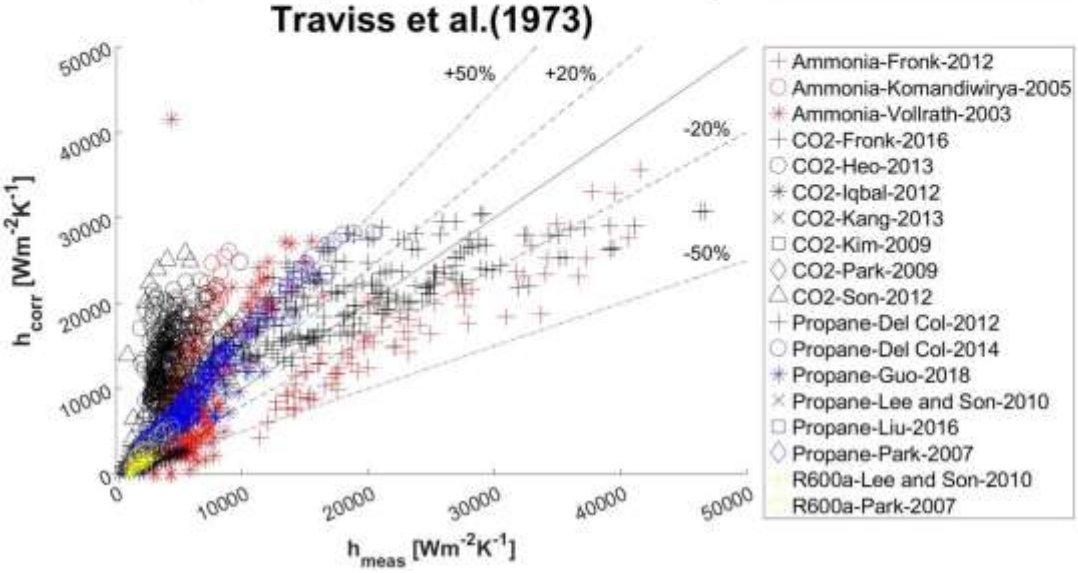
Traviss et al.(1973)
+50%
+20%
-20%
-50%
h_corr [Wm^-2K^-1]
h_meas [Wm^-2K^-1]
Ammonia-Fronk-2012
Ammonia-Komandiwirya-2005
Ammonia-Vollrath-2003
CO2-Fronk-2016
CO2-Heo-2013
CO2-Iqbal-2012
CO2-Kang-2013
CO2-Kim-2009
CO2-Park-2009
CO2-Son-2012
Propane-Del Col-2012
Propane-Del Col-2014
Propane-Guo-2018
Propane-Lee and Son-2010
Propane-Liu-2016
Propane-Park-2007
R600a-Lee and Son-2010
R600a-Park-2007

Figure B.1 Predicted and experimentally-reported flow condensation from smooth tubes with natural refrigerants, with predictions calculated from a) Cavallini et al. [83], Cavallini et al. [85], and Kim and Mudawar [35]; b) Shah [34], Shah [84], Shah [68], and Shah [67]; and c) Akers et al. [87], Macdonald and Garimella [89], and Traviss et al. [69] correlations.

a

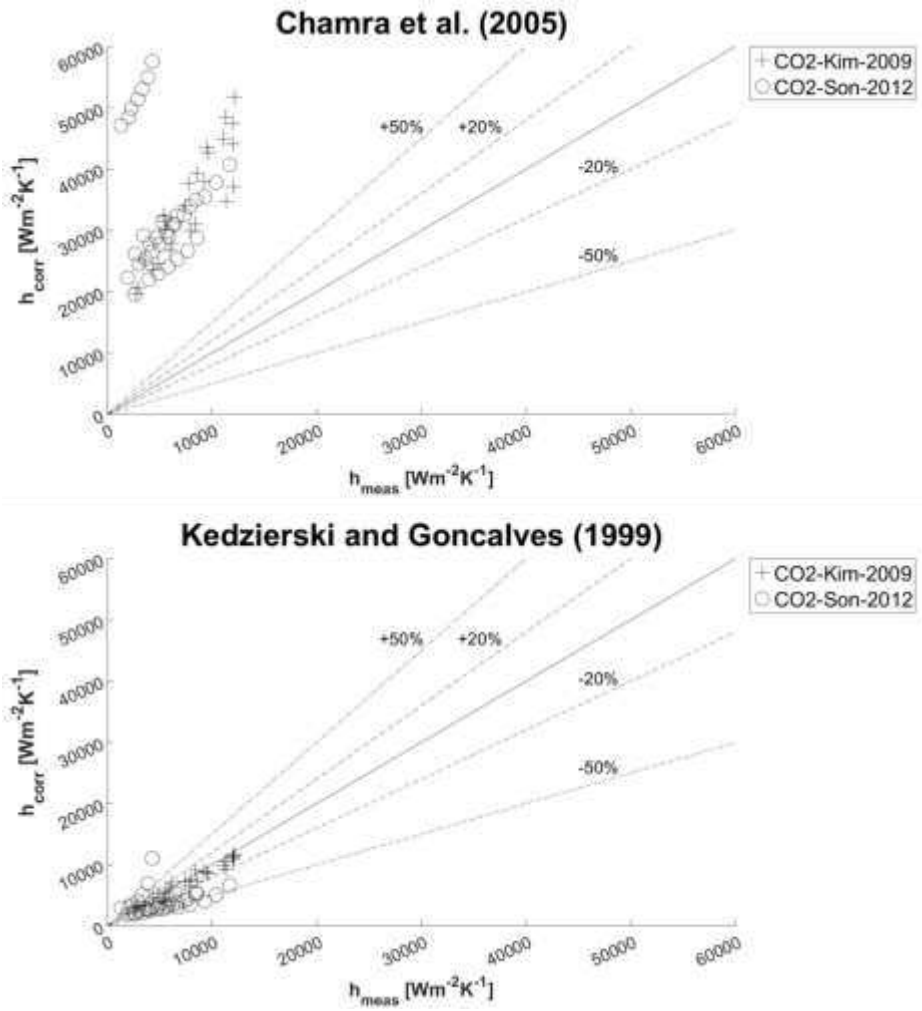

Figure B.2 Predicted and experimentally-reported flow condensation using natural refrigerants in enhanced tubes, with predictions calculated from Chamra et al. [77] and Kedzierski and Goncalves [57]